# MICROFLUIDIC DROPLET ARRAYS FOR HIGH-THROUGHPUT SCREENING OF MICROALGAE

TSOI CHI CHUNG

PhD

The Hong Kong Polytechnic University

2024

The Hong Kong Polytechnic University

Department of Applied Physics

# Microfluidic Droplet Arrays for High-Throughput Screening of Microalgae

TSOI Chi Chung

A thesis submitted in partial fulfilment of the requirements for the degree of Doctor of Philosophy

Dec 2022

# Certificate of Originality

I hereby declare that this thesis is my own work and that, to the best of my knowledge and belief, it reproduces no material previously published or written, nor material that has been accepted for the award of any other degree or diploma, except where due acknowledgement has been made in the text.

_____(Signature)

_____TSOI Chi Chung_____ (Name of candidate)

# Dedication

I dedicate my dissertation work to my family. A special feeling of gratitude to my loving parents. At the same time, I want to thank my girlfriend, Miss Wing Yan CHENG. Although we don't know whether we can continue our relationship in our lifetime, I also want to thank her for her accompany during the study.

I would like to deeply thank **Dr. Qingming CHEN** (Sun Yat-Sen University) for his moral support when I feel lost in the study. Also, I would like to thank Prof. Jianhua HAO (PolyU, AP). He taught me what is **"Fishing is much more than fish"** (授人以魚不如授人以漁). And that wording helping me a lot in the doctorate study and the future.

Finally, I would like to thank myself. Doctorate study is just like hiking. Doctoral study is only the starting point of a research career, like being led by a guide to climb to the top of first mountain. But in fact, there are many mountains in the world. In my doctoral degree, I climbed to the top of this mountain, but there are still many, many mountain tops that have not been surmounted. Even if I climbed to the top of this mountain, I do not have a must to go to the tops of other mountains on the road of research. Selling hiking equipment at the foot of the mountain and assisting others to climb the mountain also contribute to the development of hiking.

# Abstract

Microalgae are rich in special nutrients such as lipids, polysaccharides, and unsaturated fatty acids (DHA, EPA). They hold great promise as new resources for health foods, nutraceuticals and biofuels. The selection of highly-productive species is crucial to the commercial success (ingredients, productivity, cost) of microalgae. The prevailing methods often use large bioreactors to grow microalgae and have the drawbacks of intensive labour work, long time (typically 6 months) and low success rate. On the other hands, microfluidics has seen great success in drug screening using mammalian cells. Similarly, microfluidics may be a powerful solution to screening microalgal cells.

This PhD research aims to develop novel microfluidic techniques for high-throughput screening of gene-mutated microalgal species, particularly in two parts: (1) a novel design to form a large array of single microalgal cells that allows to electrically manipulate any individual cell (called *addressable XY array*); and (2) a new method to form large number of droplets that contain microalgal cells (called *EWOD templated pressing method*). Both are original ideas and enabling techniques for microalgal screening, with high scientific novelty and strong application prospects.

In one part of this study, a unique design called electrically-addressable microfluidic XY array (in short, XY array) is developed to form a large array (16×16) of microalgal cells for high-throughput screening. The XY array arranges $N$ parallel electrode lines (called X lines) on the top and another $N$ lines (called Y lines) on the bottom to form an $N \times N$ array of microalgae and to use AC electric signals and thus dielectrophoretic force to control the trap and release of any individual microalgal cell

at any specific unit of the XY array. Particularly, this XY array needs only $2N$ electrode lines to manipulate $N^2$ cell units and is thus more suitable for large array and high throughput (e.g., 1,000 × 1,000).

In the other part of this research, an original EWOD templated pressing method is developed to form a large number of pL droplets (e.g., $10^5$) in batch using photo-patterned SU-8 microwells fabricated on an ITO glass slide as the template. Compared to previous literature, which achieved production rates of less than 10%, this chip demonstrates an impressive production rate of over 95% in generating more than $10^6$ droplets of 0.9 pico-litres in one batch. In addition, this method could be used to generate smaller droplets with the volume of femto-litres or even atto-litres.

In summary, this PhD study has developed two enabling techniques to select the best few highly-productive species from a large number of gene-mutated microalgal cells in a more controllable and automatic manner. They would cut short the screening time from about 6 months using the current manual methods to about 2 weeks, and would drastically increase the success rate (the best 10 from $10^4$ cells). This work would promote the research and development and microalgae and expand to other applications that use an array of microparticles, such as drug screening, stem cell differentiations and bacterial studies.

# List of Publications

Journal publications

1. **Chi Chung Tsoi**, Xuming Zhang. "Microfluidic platform for microalgae screening and growth study," (under revision)
2. **Chi Chung Tsoi**, Xuming Zhang. "Digital microfluidics chip with XY microarray for microalgae culturing," (under revision)
3. **Chi Chung Tsoi**, Xiaowen Huang, Polly H.M. Leung, Ning Wang, Weixing Yu, Yanwei Jia, Zhaohui Li, and Xuming Zhang. "Photocatalytic ozonation for sea water decontamination," *Journal of Water Process Engineering*, vol. 37, p. 101501–, 2020, doi: 10.1016/j.jwpe.2020.101501.
4. Yujiao Zhu, Fengjia Xie, Tommy Ching Kit Wun, Kecheng Li, Huan Lin, **Chi Chung Tsoi**, Huaping Jia, Yao Chai, Qian Zhao, Benedict Tsz-woon Lo, Shao-Yuan Leu, Yanwei Jia, Kangning Ren, Xuming Zhang. "Bio-Inspired Microreactors Continuously Synthesize Glucose Precursor from CO2 with an Energy Conversion Efficiency 3.3 Times of Rice," *Advanced Science,* p. 2305629, 2023, doi: 10.1002/advs.202305629
5. Fengjia Xie, Huaping Jia, Ching Kit Tommy Wun, Xiaowen Huang, Yao Chai, **Chi Chung Tsoi**, Zhefei Pan, Shunni Zhu, Kangning Ren, Tsz Woon Benedict Lo, Yujiao Zhu, Xuming Zhang. "Dual-Defect Abundant Graphitic Carbon Nitride for Efficient Photocatalytic Nicotinamide Cofactor Regeneration," *ACS Sustainable Chemistry & Engineering*, vol. 11, no. 30, p. 11002-11011, 2023, doi: 10.1021/acssuschemeng.3c00361
6. Jia, Huaping, Yat Lam Wong, Aoqun Jian, **Chi Chung Tsoi**, Meiling Wang, Wanghao Li, Wendong Zhang, Shengbo Sang, and Xuming Zhang.

"Microfluidic Reactors for Plasmonic Photocatalysis Using Gold Nanoparticles," *Micromachines (Basel)*, vol. 10, no. 12, p. 869–, 2019, doi: 10.3390/mi10120869.

7. Chen, Qingming, Xiliang Tong, Yujiao Zhu, **Chi Chung Tsoi**, Yanwei Jia, Zhaohui Li, and Xuming Zhang. "Aberration-free aspherical in-plane tunable liquid lenses by regulating local curvatures," *Lab on a chip*, vol. 2, no. 5, pp. 995–11, 2020, doi: 10.1039/c9lc01217f.
8. Jia, Huaping ; Wong, Yat Lam ; Wang, Bingzhe ; Xing, Guichuan ; **Tsoi, Chi Chung** ; Wang, Meiling ; Zhang, Wendong ; Jian, Aoqun ; Sang, Shengbo ; Lei, Dangyuan ; Zhang, Xuming. "Enhanced Solar Water Splitting Using Plasmon-Induced Resonance Energy Transfer and Unidirectional Charge Carrier Transport." *Optics express*, vol. 29, no. 21, pp. 34810–34825, 2021, doi: 10.1364/OE.440777.
9. Zhu, Yujiao, Qingming Chen, **Chi Chung Tsoi**, Xiaowen Huang, Abdel El Abed, Kangning Ren, Shao-Yuan Leu, and Xuming Zhang. "Biomimetic reusable microfluidic reactors with physically immobilized RuBisCO for glucose precursor production," *Catalysis science & technology*, vol. 12, no. 16, pp. 59–52, 2022, doi: 10.1039/d1cy02038b.

Conference publications

1. Huaping Jia, **Chi Chung Tsoi**, Wendong Zhang, Aoqun Jian, and Xuming Zhang, "Efficient Photocathode Combining Surface Plasmon Resonance Effect with Hole Transport Layer in Visible Light," in *26th Optoelectronics and Communications Conference*, P. Alexander Wai, H. Tam, and C. Yu, eds., OSA Technical Digest (Optica Publishing Group, 2021), paper W4C.4., doi:

10.1364/OECC.2021.W4C.4

Patents

1. Xuming Zhang, **Chi Chung Tsoi**, A microfluidic chip based on dielectrophoresis/electrowettering, China Patents of Invention, Application No. 201910479720.3 (张需明, **蔡智聪**, 一种基于介电电泳/电浸润效应的微流芯片, 发明专利, 授权公告号 CN 110193386 B 授权公告日 2021.07.20)
2. Xuming Zhang, Heng Jiang, **Chi Chung Tsoi**, A microlens, Chinese Patent of Invention, Application No. CN202211263574.9 (张需明, 姜衡, **蔡智聪**, 一种微透镜, 发明专利, 授权公告号 CN115437045B 授权公告日 2022.08.15)
3. Xuming Zhang, Heng Jiang, **Chi Chung Tsoi**, An artificial compound eye imaging system, Chinese Patents of Invention, Application No. CN202211235265.0 (张需明, 姜衡, **蔡智聪**, 一种人工复眼成像系统, 发明专利, 授权公告号 CN115717933A 授权公告日 2023.02.28)
4. Xuming Zhang, Heng Jiang, **Chi Chung Tsoi**, A connection method between optical fiber and microlens, Chinese Patent of Invention, Application No. CN202211263511.3 (张需明, 姜衡, **蔡智聪**, 一种光纤与微透镜的连接方法, 发明专利, 授权公告号 CN115437067A 授权公告日 2022.12.06)

# List of Awards

1. **Dr Winnie S M Tang-PolyU Student Innovation and Entrepreneurship Scholarship**, PolyU Student Entrepreneurial Proof-of-Concept (POC) Funding Scheme, Knowledge Transfer and Entrepreneurship Office, The Hong Kong Polytechnic University, 2023
2. **Micro Fund Top Performers award**, Micro Fund Scheme, Knowledge Transfer and Entrepreneurship Office, The Hong Kong Polytechnic University, 2023

# Acknowledgments

This thesis would not have been completed without help and support from many people.

First and foremost, I would like to express my sincerest appreciation to my chief supervisor, **Prof. Xuming ZHANG**. Without his excellent guidance, valuable suggestions, patient encouragement and continuous support during the past three years of my Ph.D study, it would be impossible for me to complete my research work. His high standard, profound academic insight and inspired discussions contribute greatly to improving the quality of my doctorial research. Also, I would like to thank Dr. Yanwei JIA (University of Macau) and Dr. Xiaowen HUANG (Qilu University of Technology) for their suggestions and support to me at the beginning of my Ph.D study. At the same time, I thank all my group members for their great help during my Ph.D. study, including Dr. Yujiao ZHU, Dr. Huaping JIA, Dr. Fengjia XIE, Miss Yuhui LIU and Mr. Heng JIANG.

Besides, I would also like to heartfelt thank **Mr. Kai Hong HO** (PolyU, AP) for his great assistance and excellent hand-work device on my postgraduate research. Furthermore, I would like to thank Dr. Terence WONG (PolyU, UMF) for his technical support.

Last but not least, I would like to thank Mr. Chung Pok CHU (PLKLSP) that assisted me in setting up electronic control systems of this project.

# Table of Contents

# List of Figures

# List of Tables

# Chapter 1 Introduction

## 1.1 Background

The miniaturization of laboratories down to a single chip has long been an objective in the research and testing sector. Various fields, including biotechnology, detection technology, microbial cultivation, and cancer medication screening, have accelerated the research and development of microfluidic chips. During the course of this doctoral degree program, the global outbreak of the new coronavirus in 2019 has highlighted the urgent need for virus detection technologies. Microfluidic chips offer the potential for faster and more accurate virus identification. These chips integrate multiple standard laboratory procedures, such as liquid segmentation [1]–[3], rapid PCR [4]–[6], and concentration gradient adjustments of various medications, onto a single chip, serving as a platform for virus detection [7], [8] and related medical examinations [9]. This simplifies manual operations, reduces the likelihood of errors, and standardizes the overall inspection process. Several similar chips have been developed and utilized, including those for the detection of the 2019 coronavirus [7], [10]–[13], microalgae species screening, and microalgae breeding condition research. Notably, many of these chips outperform human macroscopic manipulation in terms of repeatability, error rate, and reaction time, such as the breast cancer medication

screening chip [14]–[16]. Apart from the aforementioned benefits, the ability to perform droplet digital microfluidics in a high-throughput format not only enhances detection comprehensiveness (from analog to digital) but also offers a more digital approach (using the same sample for simultaneous detection of multiple projects).

Digital microfluidics is a technology derived from continuous microfluidics and can be considered a branch of it. Unlike continuous microfluidics, digital microfluidics operates with droplets instead of continuous fluids, which is its main distinction. It combines micro (nano) nanotechnology, engineering, material science, physics, chemistry, and biology, similar to continuous microfluidics. However, digital microfluidics requires structures for droplet generation during liquid pretreatment since it is based on discrete droplets. In terms of chip operation, both digital and continuous microfluidics involve similar processes, such as liquid pretreatment (to prevent channel clogging) and peripheral pumping (to facilitate fluid flow within the channels). Additionally, effective control methods are necessary to manipulate droplets individually in high-throughput experiments.

The development of droplet digital microfluidics marks a new chapter in microfluidics. In the past, each channel of microfluidic technology could only accommodate a single experiment at a time, limited to continuous fluid flow. Consequently, despite the benefits of high throughput and speed [17], microfluidic technology has not been fully

proven. The presence of air bubbles in the channels that require elimination poses a significant challenge. Moreover, utilizing traditional microfluidic technology as an experimental platform only allows analog representation of findings, which is incompatible with the digital world we live in today. Therefore, there is a need for further technological advancements. Continuous microfluidics lacks the capability to manipulate droplets on the chip or generate droplets, and these features require improvement.

Techniques for manipulating droplets can be broadly categorized into two groups: pushing droplets and pulling droplets. Methods for pushing droplets often involve applying heat to one side of the droplet to generate small bubbles that propel the droplet to the other side. Different heating approaches, such as laser heating or electric current passing through a coil, can be utilized. However, these techniques have the drawback of requiring temperature changes, which may hinder the handling of temperature-sensitive substances in the droplet. Manipulation of droplets by pulling force typically relies on exploiting differences in surface tension to transfer the droplets to more hydrophilic locations. Techniques such as dielectrophoresis (DEP), optoelectrowetting [18] and electrowetting on dielectric (EWOD) [19], [20] reduce localized surface tension, causing the droplets to move in the desired direction. In some cases, a hydrophobic layer may be pre-coated on the surface to maximize the difference in

surface tension. Additionally, magnetic materials can be introduced into the droplet, and a magnetic field can be applied to the corresponding area on the chip to pull the droplet to the desired location. Among these methods, DEP is the most widely used control method as it minimally affects the droplet composition. However, when conducting high-throughput experiments, the requirement for numerous electrodes may make it impractical in certain scenarios.

The techniques for droplet formation can be categorized into three main types: Y (or T) junction [21], cutting [22], [23], and jetting [24]. The first generation of digital microfluidic chips for droplet formation employed Y (or T) junctions, where one port supplied the liquid of interest while the other ports supplied liquid in other phases. The most common mixtures involved water-in-oil and oil-in-water. The second type of droplet formation involves cutting large droplets into smaller ones. As the liquid flows through the chip, it is divided to form tiny droplets. However, the first two approaches are limited by the high surface tension of water, making it difficult to generate droplets smaller than 30 pL (corresponding to spherical water droplets with a diameter of about 40 μm) [21]–[24]. Jetting is a more recent method for creating small droplets. It involves the ejection of small droplets by rapidly changing the electric field. Unfortunately, the relationship between the applied electric field and droplet volume remains unknown.

Furthermore, with global warming and irregular weather patterns, the world is currently facing or beginning to experience a food crisis. Microalgae, which are rich in protein, lipids, and other essential nutrients, offer a potential solution. Additionally, microalgae have relatively minimal environmental requirements, leading some governments to explore their potential as future food sources. However, only 40,000 microalgae species are currently recognized worldwide [25], and experts estimate that there could be between 30,000 and over 1 million species [26], some of which may be harmful to humans, specific to freshwater or seawater environments, or possess unique survival conditions. Therefore, comprehensive research on microalgae taxonomy and associated living conditions is highly beneficial. However, such studies often require cultivating algae in large biological incubators, which can take weeks or even months. Furthermore, if the culture becomes infected with bacteria, the entire experiment must be restarted. Droplet digital microfluidics holds particular significance in the classification and screening of microalgae, as well as the formation and culture of living conditions, as it treats each droplet as an individual entity and simplifies the process.

The next section will outline the goals, objectives, and structure of this thesis.

## 1.2 Motivation

The importance of future food sources has grown considerably, driven by factors such as global warming and the prevailing food crisis. Microalgae have emerged as a

promising food source due to their short life cycle and abundance of essential nutrients for human sustenance. However, the vast number of microalgae species presents a challenge for scientists to comprehensively examine and categorize them individually. The primary aims of this research program are to classify and analyze microalgae utilizing droplet digital microfluidics and relative study.

## 1.3 Objectives

The existing droplet digital microfluidics technology lacks a reliable control approach for individually manipulating high-throughput droplets. Furthermore, the creation of consistently sized droplets with a diameter of less than 10 μm is crucial for droplet manufacturing, particularly considering the small size of microalgae (with an average diameter of less than 10 μm when measured as spheres). Therefore, this research program has two main objectives:

A. Enhance the foundation of DEP to enable its application in high-throughput droplet manipulation.

B. Develop a technique capable of consistently generating droplets with a diameter of less than 10 μm.

By achieving these objectives, the research aims to advance the field of droplet digital microfluidics and facilitate the classification and analysis of microalgae using this technology.

## 1.4 Organization of thesis

This thesis is structured into six parts, as follows:

Introduction

This section provides an overview of the research's historical background, addresses the current global issues, discusses the challenges faced by related scientific research programs, and highlights the significance of the specific research project.

Literature review

In this section, a comprehensive review of previous scientific studies related to digital microfluidics and microalgae is presented. It includes an examination of previous research on microalgae classification using digital microfluidics and the investigation of optimal microalgae production conditions. Additionally, the literature review analyzes the current trends and advancements in allied disciplines.

Methodology

The methodology section provides a brief introduction to the instruments used in the experimental part of the project, along with their specific usage methods and parameters.

XY array

This section focuses on the development of an XY array based on DEP principle. The XY array reduces the number of electrodes required in the high-throughput droplet chip, enabling control of the number of X multiplied by Y units using X plus Y electrodes.

Droplet generation

This part discusses the combination of microstructure and DEP principles to break the surface tension of water and generate small, consistent droplets as small as 0.9 pL.

Future works and conclusion

The final section summarizes the entire study plan, discusses the limitations and shortcomings of the research, and outlines the future research directions based on the findings of this study.

By organizing the thesis in this manner, the research aims to provide a comprehensive introduction, review of literature, methodology, and experimental findings, ultimately concluding with future research prospects and implications.

# Chapter 2 Literature Review

## 2.1 Introduction

Microalgae are rich in various biochemical elements, including proteins, carbohydrates, lipids, pigments, carotenoids, and valuable chemicals. These components have led to the exploration of microalgae as feedstock for biopharmaceuticals, cosmetics, nutraceuticals, functional foods, and biofuels [27]–[29]. Microalgae biomass offers the potential for multi-valorization in biorefinery settings, enabling the production of diverse biofuels and high-value biotechnological products. Furthermore, microalgae perform photosynthesis, which leads to the simultaneous generation of oxygen and reduction of $CO_2$.

In light of concerns regarding climate change and the depletion of fossil fuel resources, there has been increased interest in sustainable biofuel production, which has propelled microalgae to the forefront as potential renewable biofuel sources. The bioproduction of specialized and high-value compounds using microalgae has also gained attention due to the growing demand for environmentally friendly and sustainable manufacturing practices. Consequently, there is a growing scientific and commercial interest in microalgae. However, the ideal growth conditions for many microalgae species are still unknown, hindering their full exploitation. To unlock the potential of microalgae,

researchers have explored various approaches. Strain selection, development, and culture are the three primary steps in microalgae bioproduction. However, these stages are time-consuming, labor-intensive, expensive, and low in throughput due to their reliance on large-scale equipment and complex procedures [30].

Since the 1980s, researchers have been utilizing microfluidics to address these challenges. Microfluidic lab-on-a-chip systems offer several advantages over traditional methods and have the potential to revolutionize microalgal culture and handling technologies, thereby advancing microalgal biofuel/bioproduct research [31]. Microfluidics allows for the manipulation, monitoring, and control of extremely small sample volumes at the nL to pL scale. It enables processing and analysis at the single-cell resolution with high precision, and these operations can be conducted in a massively parallel manner, facilitating high-throughput experiments at a lower cost [32]–[34]. Given the microscopic size and diluted culture of microalgae, the use of microfluidic-based devices for both fundamental research and industrial applications in microalgae is becoming increasingly crucial. Microfluidic-based devices surpass traditional techniques in sorting and analyzing small sample volumes (ranging from nL to pL) with high sensitivity. They also offer the flexibility to mimic the natural environments of live cells. State-of-the-art techniques need to be employed to enhance productivity, quality, and economic aspects of both upstream and downstream

operations.

This study aims to outline recent advancements and future directions in microfluidic systems for microalgal biotechnology applications. **Figure 2.1** provides a diagrammatic representation of the review study. The review material is structured similar to the rollers in a peristaltic pump.

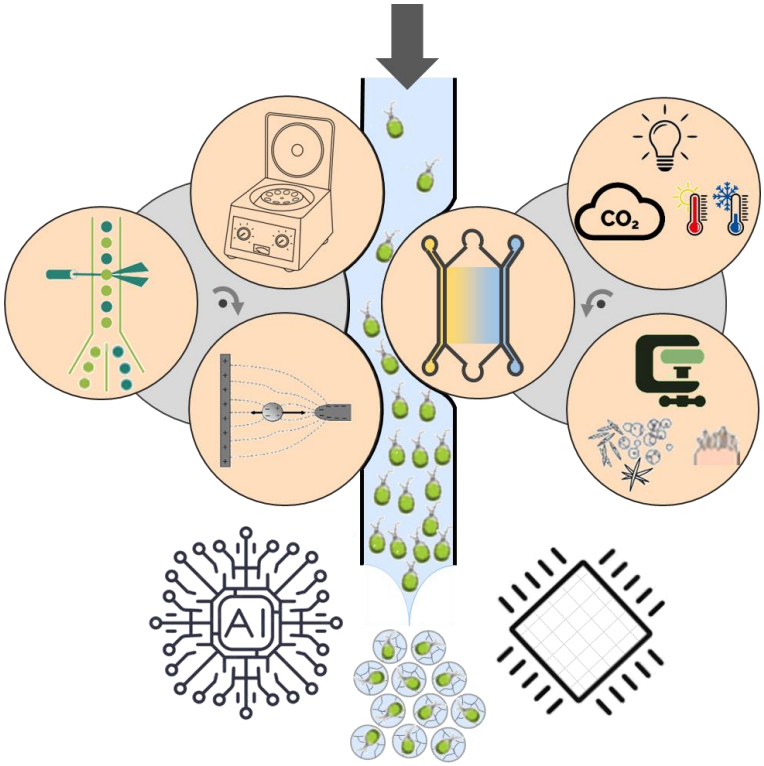


**Figure** 2.1 Diagrammatic representation of this review study.

The first section of this chapter focuses on the microfluidic platform for microalgal screening. It covers topics such as algae concentration, screening of lipid algae at various concentrations using techniques such as DEP and EWOD and flow cytometry

with Raman spectrum analysis, and cutting-edge screening applications involving ultrasound and piezoelectric materials. Following that, we delve into microfluidic applications for microalgal monitoring and growth optimization, including the creation of one-dimensional (1D) and two-dimensional (2D) concentration gradients, temperature control, light intensity control, exploration of novel growth conditions such as mechanical stress and growth in droplets, and a review of hydrogel as a growth medium for microalgae. The chapter concludes by discussing current limitations and outlining potential future prospects for microfluidics technology.

## 2.2 Microfluidic platforms for microalgal screening

Microalgae present promising opportunities to replace petroleum-based fuels and provide valuable nutrients, leading researchers to explore methods for batch cultivation to maximize the extraction of high-value compounds.

In recent years, droplet-based microfluidic systems have revolutionized the genetic engineering of microalgae, significantly improving the production of valuable compounds. These systems enable the study of hundreds to thousands of individual cells under precisely controlled conditions [35]–[37]. Each pL or nanoliter microdroplet acts as an independent microreactor, allowing multiple chemical and biological tests to be conducted simultaneously under diverse cell growth conditions. Studies have successfully demonstrated the isolation and cultivation of individual microalgal cells

using microdroplets, facilitating the identification of suitable cells for biotech feedstocks [38], [39]. However, the production of droplets does not guarantee the presence of microalgae in every droplet, making the best-case scenario to have one living cell per droplet for maximal production. Traditional methods of microalgae concentration, such as microcolumn or pore filtration, have faced challenges in terms of microalgae survival rates.

A novel approach to microalgae concentration involves monitoring the presence or absence of microalgae and subsequently separating them individually. Chlorophyll fluorescence is a common and sensitive method for detecting microalgae presence, but additional fluorescent markers can also be employed [40]. For instance, fluorescent dyes can stain the neutral lipids of microalgae. Although fundamental genetic engineering tools, including selectable markers, reporter genes, and promoter elements, are available [41]–[43], the isolation of a single strain remains a slow and cumbersome process. Therefore, efficient isolation and analysis of strains or droplets continue to be labor-intensive and time-consuming. Consequently, rapidly screening each droplet for the presence of microalgae has become a primary challenge in cultivating microalgae using droplet microfluidic systems. Furthermore, identifying and collecting microalgae with high concentrations of lipids or other valuable compounds after cultivation is crucial for the future scalability of microalgae production in conjunction with droplet

microfluidics. Finally, innovative and less explored research combining microalgae culture with droplet microfluidics will be discussed.

By reorganizing and enhancing the logical flow of the literature review section, the focus is on the utilization of microfluidic platforms for microalgal screening, with an emphasis on trapping and releasing individual cells. This revised version aims to provide a more engaging and cohesive presentation of the topic, highlighting the advancements in droplet-based microfluidics and addressing key challenges in microalgae cultivation, concentration, and identification.

### 2.2.1 Concentrating algae

Concentrating microalgae is a crucial step in various applications, such as microalgal biotechnology and biofuel production. Traditional methods like microcolumn or pore filtration have limitations, especially when live cells need to be preserved. However, innovative microfluidic approaches offer promising solutions for efficient algae concentration.

In droplet-based microfluidic systems, two main strategies are employed for concentrating microalgae:

a) Separating Droplets with Cells: This approach involves generating droplets first and then isolating the droplets containing microalgae cells. One method focuses on generating droplets from a low-concentration microalgae cell solution, resulting in

some droplets lacking microalgae or containing only a single cell. After cultivation, these droplets are screened to identify those with microalgae. Ming, Li et al. developed a sorting platform using hydrogel droplets for microalgae concentration [44]. They demonstrated the use of hydrogel droplets that shrink as microalgae cells proliferate, enabling passive sorting based on droplet size using inertial microfluidics. Inertial microfluidics employs inertial lift forces to direct droplets of different sizes to equilibrium positions along the fluid streamlines. This approach provides high-throughput sorting of hydrogel droplets in oil solutions. Li also showcased the collection of shrunken cells with high purity by remove empty hydrogel droplets, highlighting the potential for combining genetic engineering with active sorting techniques.

b) Concentrating Microalgae before Droplet Formation: This strategy involves concentrating microalgae first and then forming droplets from the concentrated cell solution. By accumulating and concentrating microalgae cells through particle interactions, device structures, and flow profiles, droplets with a higher probability of containing multiple microalgae cells are produced. Ziyi, Yu et al. demonstrated this approach using electrophoresis to separate droplets containing microalgae cells [45]. They encapsulated single cells of distinct marine microalgae species in pico-liter-sized droplets and employed an enhanced laser-induced fluorescence technique for droplet-

based microfluidics. This method enables high-throughput microalgae analysis and screening, offering potential applications in various processes.

Furthermore, Shakeel Syed et al. developed a novel lab-on-a-chip system for microalgal cell collection using the hydrocyclone concept [46]. Hydrocyclones are simple, reliable devices with no moving parts. By utilizing multi-jet 3D printing technology, small vertical cyclones were designed for efficient particle-liquid separation. The design specifications of a hydrocyclone, such as the diameter of the cylindrical section, significantly influence its performance. This innovative approach shows promise for concentrating microalgal cells in low-concentration solutions.

Concentrating algae is a critical step that enhances the efficiency and throughput of microalgae-related applications. These novel microfluidic techniques, including droplet-based sorting platforms, electrophoresis-based separation, and hydrocyclone-based concentration, offer innovative solutions for concentrating microalgae and hold potential for further advancements in the field.

### 2.2.2 Screening different concentration of lipid algae by DEP

The extraction of oil from microalgae is a key area of research due to their fast growth rate and high-value substances, such as DHA. Before extracting oil, it is essential to identify and separate microalgae cells with a high concentration of lipids. In this section, we will explore two modern methods for distinguishing microalgae cells

based on their lipid content: dielectric parameters and morphological and electromagnetic wave absorption rate analysis.

DEP is a technique that exploits the differences in dielectric parameters of matter to detect and isolate microalgae cells containing a large amount of lipids within droplets. The working principle of DEP in droplet microfluidics is akin to that of capacitors. When droplets with different dielectric constants are exposed to an electric field, forces are generated that cause the droplets to move towards or away from regions of high electric field strength.

To distinguish microalgae cells based on lipid content, droplet microfluidics can manipulate droplet movement by leveraging DEP forces. The force exerted on the droplets can be calculated as following equation [47]:

$$< F_{DEP} > \; = \; \pi \, \varepsilon_m \; a^3 \, Re \left[ \frac{\tilde{\varepsilon}_p - \tilde{\varepsilon}_m}{\tilde{\varepsilon}_p + 2 \, \tilde{\varepsilon}_m} \right] \nabla \, |E|^2 \qquad (2.1)$$

where a represents radius of the droplet or particle, $\varepsilon_m$ represents the dielectric constant of the surrounding medium, $\varepsilon_p$ refers to the complex permittivity of the droplet, $Re \left[ \frac{\tilde{\varepsilon}_p - \tilde{\varepsilon}_m}{\tilde{\varepsilon}_p + 2 \, \tilde{\varepsilon}_m} \right]$ represents Clausius-Mossotti factor and E represents complex applied electric field. When the Clausius-Mossotti factor value exceeds 0.4 or falls below -0.4, it indicates sufficient force to influence the droplet's direction of movement.

When the value is greater than 0.4 or less than negative 0.4, it can be regarded as having sufficient force to affect the moving direction of the droplet.

Researchers have developed innovative DEP-based cell separation devices and platforms to effectively screen microalgae with varying lipid concentrations. Zhongle Zhang et al. presented a DEP-activated cell separation device using 3D microelectrodes and fluidic sidewalls made of Ag-PDMS [48]. The device employs interdigitated microelectrodes and sawtooth-shaped coverings to create non-uniform electric fields. This setup enables the capture and immobilization of target cells on the electrode tips, protecting them from strong fluid drag.

Another approach by Song-I Han utilizes a lateral DEP-based microfluidic platform for separating cells based on intracellular lipid content [49]. By employing a planar interdigitated electrode array, this platform takes advantage of the electric field gradient generated towards the electrode edges. The pDEP force attracts cells along the electrode edges, causing lateral displacement. The dielectric properties of cells, influenced by their lipid content, determine the strength of the pDEP force and the degree of cell displacement.

These DEP-based platforms offer various applications, including the sorting of cells based on lipid levels, the enrichment of high-lipid-producing strains, and the assessment of intracellular lipid heterogeneity. The ability to quickly screen microalgae populations for lipid content allows for informed decisions during algal biofuel production and optimization.

By harnessing DEP forces in droplet microfluidics, scientists can efficiently screen and isolate microalgae cells with high lipid concentrations, facilitating downstream processes such as oil extraction and biofuel production.

### 2.2.3 Flow cytometry with Raman

Traditional analytical instruments lack the ability to provide single-cell precision and non-invasive assessment of heterogeneous populations of microalgae cells. Flow cytometry, known for its high-throughput analysis of individual cells, has been a standard tool in large-scale cell studies. However, flow cytometry relies on single-point light scattering measurements and lacks spatial metrics for precise characterization of cellular morphology and intracellular phenotypes. Moreover, fluorescent labeling commonly used in flow cytometry interferes with the lipid production of microalgae.

To overcome these limitations, the combination of microfluidics, flow cytometry, and Raman imaging has emerged as a powerful approach. Keisuke Goda and his team have made significant contributions in this field, employing microfluidic platforms and Raman imaging to achieve high-throughput, single-cell resolution, and label-free analysis of microalgae populations.

Baoshan Guo et al. developed a platform that utilizes a mode-locked fiber laser as the light source and a Michelson interferometer setup [50]. By generating rainbow pulses, the platform enables the acquisition of 1D intensity and phase images of microalgae

cells. Rainbow pulses at different frequencies interact with the cells, encoding information about the cell's thickness, refractive index, and absorption and scattering properties. By decoding the temporal interferogram, 1D intensity and phase images are obtained, which can be stacked to generate 2D intensity and phase images as the cells flow through the microchannel. This approach provides precise cell categorization without the need for fluorescent labeling, with a low error rate of only 2.15%.

Hiramatsu Kotaro introduced the FT-CARS flow cytometer, which combines flow cytometry with a Raman imaging system [51]. In this system, fs laser pulses are used as the light source, and the optical pathway is modified to enable measurement of intracellular molecular vibrations. Pump and probe pulses are alternately generated, and the delay-dependent anti-Stokes signal, indicative of the cell's Raman spectrum, is detected and analyzed. This approach allows for high-throughput analysis of cells at scanning speeds of up to 24,000 scans $s^{-1}$, providing valuable Raman spectra for a large number of cells.

The integration of flow cytometry with Raman imaging in microfluidic systems offers a promising avenue for precise and high-throughput analysis of microalgae populations. This approach enables the assessment of intracellular phenotypes, including lipid content, without the need for fluorescent labeling, providing valuable insights for applications such as biofuel production and optimization.

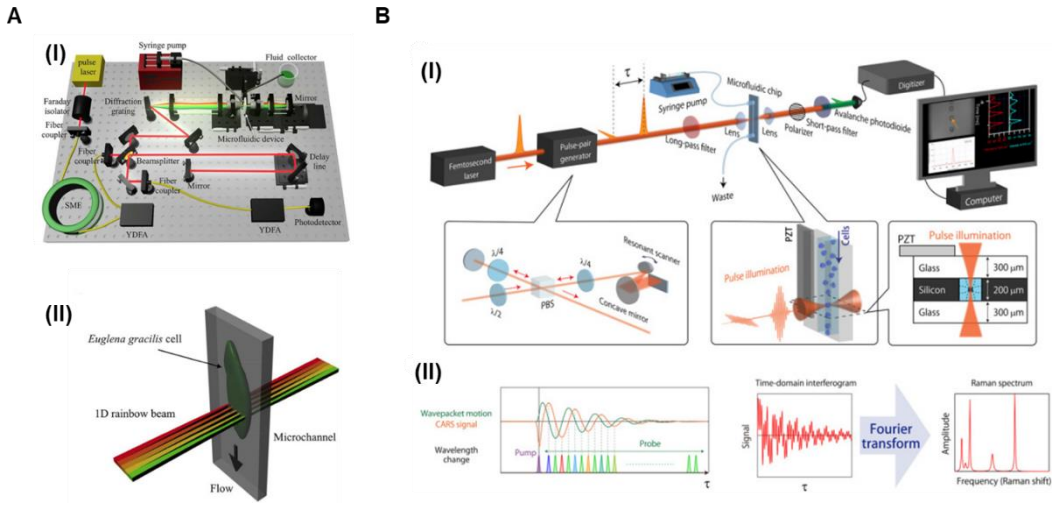


**Figure 2.2** (a) Optofluidic time-stretch quantitative phase microscope. (I) Schematic of the microscope. (II) Enlarged view of the optical interrogation region in the microchannel [50]. (b) (I) Schematic of the FT-CARS flow cytometer. (II) Principles of FT-CARS spectroscopy [51].

### 2.2.4 Other new method for screening

In addition to the conventional methods of concentrating microalgae and using DEP and cytometry for analysis and isolation, several lesser-known methods show promise for future microalgae screening applications. These innovative techniques offer unique capabilities and have the potential to replace traditional screening approaches. Let's explore three of these methods:

A. Microfluidic Impact Printing with Real-time Cellular Identification, Wang, Yiming et al. have developed a novel single-cell isolation method using microfluidic impact printing coupled with real-time cellular identification [52]. This label-free approach

enables the encapsulation of single cells in individual droplets and their precise positioning in an array configuration. The system demonstrates high efficiency and throughput, with successful encapsulation of microbeads and collection of HeLa cells. The technique has minimal impact on cellular processes and viability, making it suitable for single-cell applications such as single-cell omics, tissue engineering, and cell-line creation.

B. Flexural Wave-driven Acoustophoretic System for Particle and Cell Wall Entrapment, Aghakhani, Amirreza et al. have developed a flexural wave-driven acoustophoretic system for particle and cell wall entrapment [53]. By exciting a microscope glass slide at its resonance frequencies, flexural waves transmit acoustic energy to the microfluidic channel, allowing for the trapping of particles and cells against the soft PDMS microchannel walls. This technique provides insights into designing simple acoustofluidic devices capable of microparticle/cell wall entrapment. The study focuses on the interaction of motile cells, including microalgae, with soft barriers under ultrasonic pressures.

C. Diamagnetic Separation using Ferrofluids in Aqueous Two-Phase Systems (ATPS), Navi, Maryam et al. have introduced the use of ferrofluids in ATPS to create diamagnetically sensitive liquid-in-liquid droplets in microfluidics [70]. This technique allows for the separation of empty droplets from droplets containing

particles and cells through diamagnetic separation. The study demonstrates the successful isolation of water-in-water droplets containing particles and cells, with excellent purity and cell vitality. The microfluidic device incorporates flow focusing junctions, a larger channel for droplet separation, and an expansion and sorting zone for efficient droplet collection.

These novel screening methods offer unique capabilities for different stages of microalgae analysis. Wang et al.'s microfluidic impact printing provides efficient single-cell isolation, Aghakhani et al.'s flexural wave-driven acoustophoretic system enables particle and cell wall entrapment, and Navi et al.'s use of ferrofluids in ATPS allows for effective diamagnetic separation. These innovative techniques hold promise for advancing microalgae screening and have potential applications in various fields.

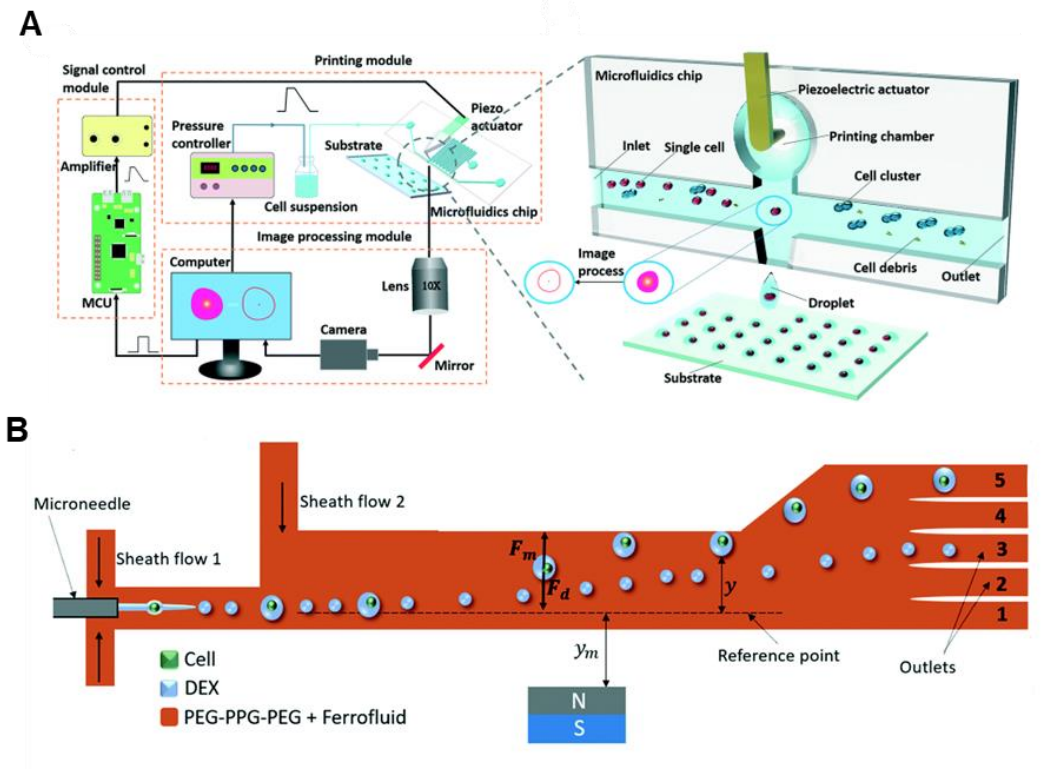


Figure 2.3 (a) Design and working principle of the single-cell isolation system [68]. (b) Schematic illustration of diamagnetic separation of cell-containing droplets from empty droplets [54].

## 2.3 Microfluidic platforms for microalgal monitoring and growth optimization

Nutrient availability plays a crucial role in microalgae cultivation, with phosphorus (P), nitrogen (N), and potassium (K) being the key nutrients of interest. Traditionally, researchers have utilized culture flasks or chemostats in the laboratory to explore the impact of various nutritional and environmental variables on microalgal

growth. Through this approach, it has been observed that the concentration and ratio of N, K, and P, as well as temperature, fluid flow, and light intensity, can significantly influence algal growth rates and compound concentrations within the algae.

However, research investigating the simultaneous effects of multiple environmental factors, particularly at the cellular level, has been limited. Conducting such experiments often requires substantial reagent quantities and time, making it challenging to screen a wide range of values for each environmental parameter and obtain a quantitative understanding, especially at the single-cell level. Consequently, there is a need for further exploration into the effects of various environmental signals.

Microfluidics offers a promising solution by enabling real-time monitoring of microalgal development and precise control over environmental conditions. It provides a high-throughput format that facilitates rapid screening of multiple environmental parameters. In this section, we will discuss the use of microfluidic chips with concentration gradient structures to study nutrient comparisons. Beyond nutrient ratios, researchers have also investigated other factors that impact the growth rate of algae and the final concentration of compounds within the algae. Furthermore, we will explore alternative research approaches that have identified optimal culture conditions, encompassing both traditional and novel methods, in microfluidic-based algae culture. By leveraging microfluidic platforms, researchers can gain valuable insights into the

effects of diverse environmental signals on microalgal growth and compound production. These advancements contribute to the optimization of culture conditions and hold promise for enhancing microalgae cultivation practices.

### 2.3.1 Concentration gradients for microalgal optimization

Microfluidics has revolutionized the study of microalgae by enabling precise control over environmental conditions and providing high-throughput platforms for screening and optimization. Within this field, microfluidic platforms with concentration gradients have emerged as valuable tools for microalgal optimization. In this section, we will discuss three research studies that utilize such platforms and highlight their common points.

Guoxia Zheng et al. developed a microfluidic series for microalgal bioassays, allowing for pretests, single compound testing, and combined compound testing [55]. Their platform incorporated an upstream dilution network and a downstream diffusible culturing module. It enabled chemical liquid dilution, diffusion, microalgal culture, and online screening. The device provided a versatile and high-throughput system for studying the effects of various compounds on microalgal growth.

Fangchen Liu et al. designed a diffusion-based array microhabitat system with stable dual chemical gradients [56]. This platform featured an array microhabitat format that offered diverse environmental conditions for photosynthetic cell development. By

studying the synergistic effects of nitrogen (N) and phosphorus (P) gradients on Chlamydomonas reinhardtii growth, they demonstrated the significance of nutrient interactions in microalgal optimization.

Marwa Gamal Saad et al. introduced a gradient microfluidic platform based on droplets to investigate the effects of nitrate concentrations on Chlorella vulgaris growth [81]. Their device encapsulated cells in droplets with varying nitrate concentrations, enabling controlled experiments with reduced reagent preparation time. By tracking chlorophyll intensity within each droplet, they gained insights into the growth kinetics of microalgae under different nutrient conditions.

These studies share a common focus on leveraging microfluidic platforms with concentration gradients to optimize microalgal growth. By precisely controlling and manipulating nutrient concentrations, these platforms allow researchers to explore the synergistic effects of multiple nutrients and identify optimal conditions for microalgal cultivation. Furthermore, the high-throughput nature of these platforms enables efficient screening of various environmental parameters, significantly reducing time and resource requirements compared to traditional methods.

In summary, microfluidic platforms with concentration gradients offer a powerful approach to study microalgal optimization. They enable fine-tuned control of nutrient conditions, facilitate exploration of nutrient interactions, and provide high-throughput

screening capabilities. These platforms contribute to advancing our understanding of microalgal growth and have the potential to drive advancements in microalgal-based applications such as biofuel production and bioremediation.

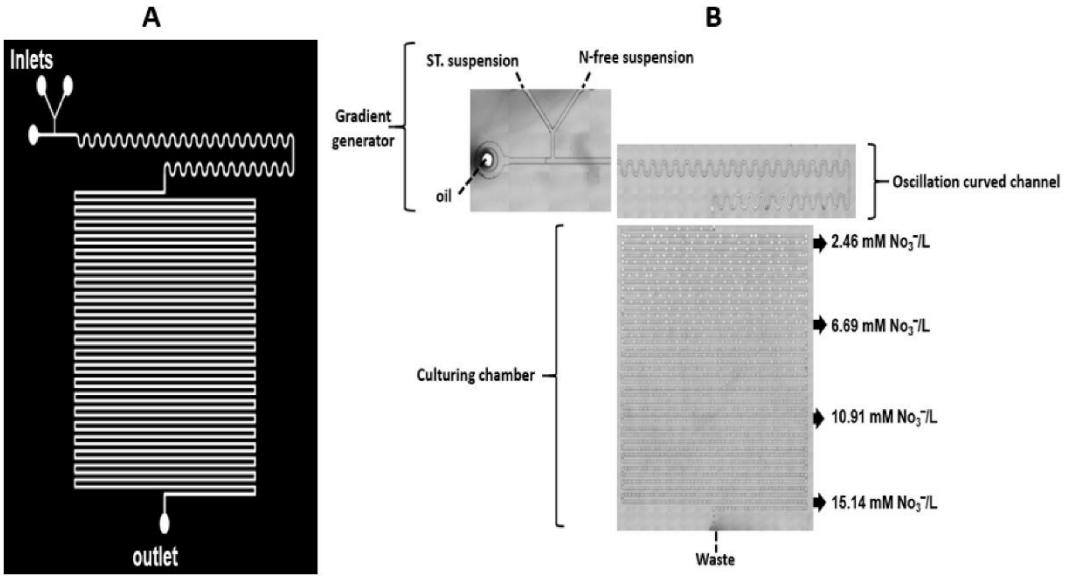


**Figure 2.4** The gradient-based microfluidic used for this experiment. (a) The master's design of the microfluidic. (b) gradient-based device parts showing the main areas and gradient generator [57].

## 2.3.2 Optimization by controlling of traditional growth conditions

In addition to nutrients and their ratios, traditional growth conditions such as temperature, light intensity, and carbon dioxide concentration play crucial roles in microalgae cultivation. Researchers have explored the optimization of these factors using microfluidic platforms, which provide precise control and real-time monitoring

capabilities. This section highlights studies that focus on optimizing microalgal growth by controlling and monitoring traditional growth conditions.

One study conducted by Martin Andersson et al. developed a temperature control system integrated with microfluidic devices [82]. Their approach involved placing the microfluidic chip on a thermal management stage and utilizing active liquid cooling to achieve spatiotemporal thermal modulation. By dynamically adjusting the temperature, researchers could investigate the photophysiological changes and stress tolerance of microalgae under different thermal conditions.

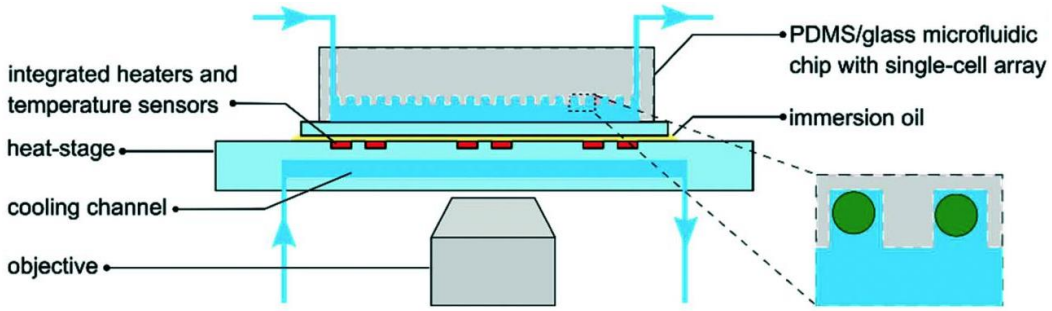


**Figure 2.5** A programmable temperature regulation system with an attached microfluidic chip. Cross-section of the temperature regulation system placed under a microscope with a mounted microfluidic chip [58].

Another study by Marwa Gamal Saad et al. designed a microfluidic device to examine the relationship between light intensity and Chlorella vulgaris growth [59]. By culturing cells under varying light intensities, they observed that higher light intensities led to

increased growth rates. The microfluidic platform allowed for parallel culturing and real-time monitoring of cell growth, providing valuable insights into optimizing light conditions for microalgal cultivation.

In a study conducted by Zhen Xu et al., a microfluidic apparatus was developed to control carbon dioxide environments during microalgal cell culture [60]. Their device incorporated a hydrophobic gas semipermeable membrane, enabling accurate detection and regulation of carbon dioxide concentrations. The microfluidic system facilitated uniform gas distribution and real-time monitoring of cell development under controlled carbon dioxide conditions.

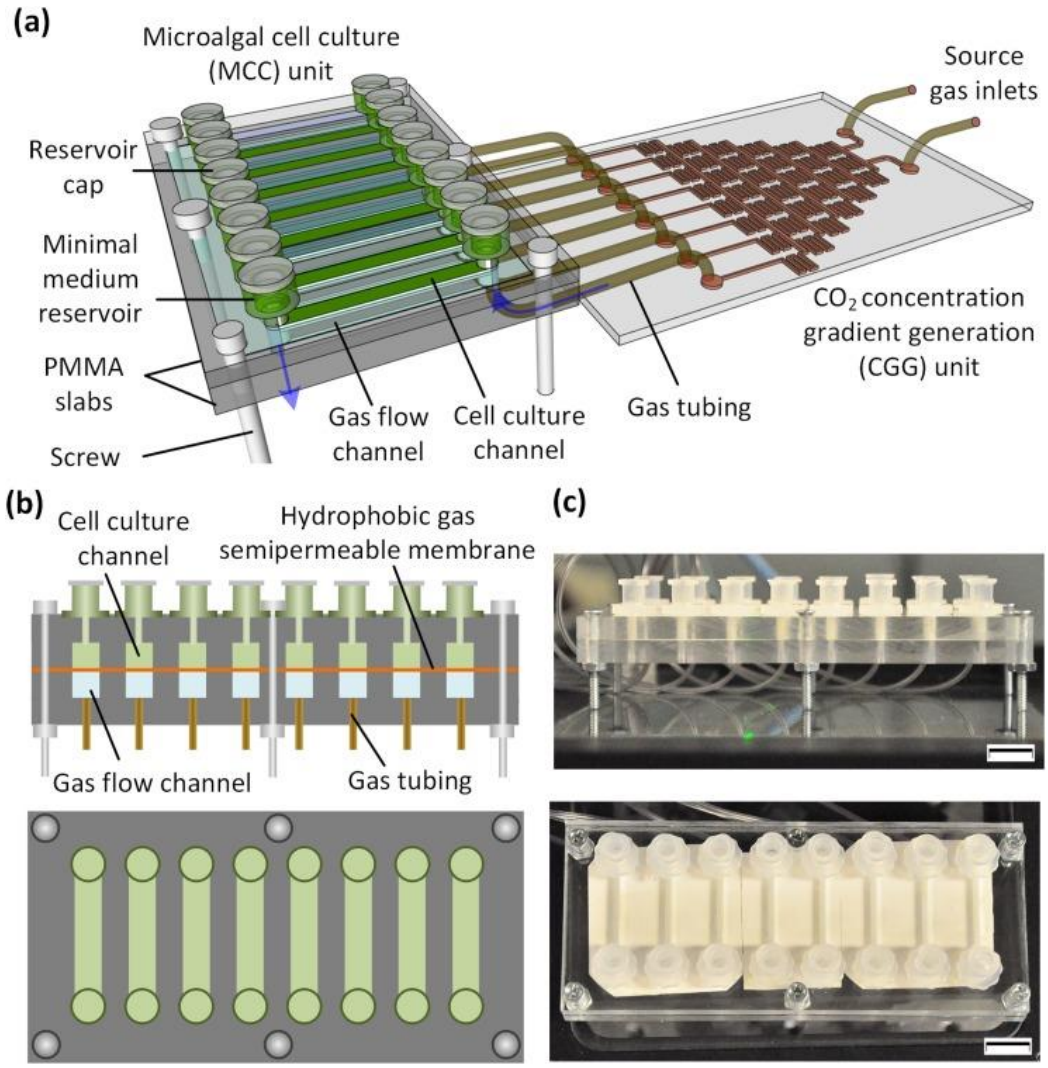


**Figure 2.6** (a) Schematic of a microfluidic device with a MCC unit and a CGG unit. (b) and (c) Side view (upper panel) and top view (lower panel) of the MCC unit [60].

These studies share a common objective of optimizing microalgal growth by controlling and monitoring traditional growth conditions. Through microfluidic platforms, researchers can precisely manipulate temperature, light intensity, and carbon dioxide concentration, gaining insights into their individual and synergistic effects on microalgal cultivation. The real-time monitoring capabilities of these platforms enable

dynamic adjustments and fine-tuning of growth conditions, ultimately leading to improved growth rates and biomass production.

In summary, microfluidic platforms offer powerful tools for optimizing microalgal cultivation by controlling and monitoring traditional growth conditions. By fine-tuning temperature, light intensity, and carbon dioxide concentration, researchers can uncover the optimal conditions for enhanced microalgal growth. These findings contribute to the development of sustainable applications such as biofuel production and bioremediation, where efficient microalgal cultivation is essential.

### 2.3.3 Optimization by controlling of other novel growth conditions

In addition to traditional growth conditions, novel approaches have been explored to further optimize microalgal growth. These approaches include controlling intracellular stress levels and exploring multicellular cultures to increase microalgal yield.

One study by Min et al. focused on applying direct mechanical stress to Chlamydomonas reinhardtii to induce lipid buildup [61]. However, traditional culture methods lacked precise control over mechanical stress application, hindering related investigations. To address this, Junyi Yao et al. developed a microfluidic device with a micropillar array to separate motile vegetative stage H. pluvialis cells from cyst stage cells and cultivate the selected cells under controlled mechanical stress [62]. Their

findings demonstrated that mechanical stress caused astaxanthin accumulation in H. pluvialis, and the microfluidic chip facilitated the screening of optimal stress levels for increased astaxanthin accumulation.

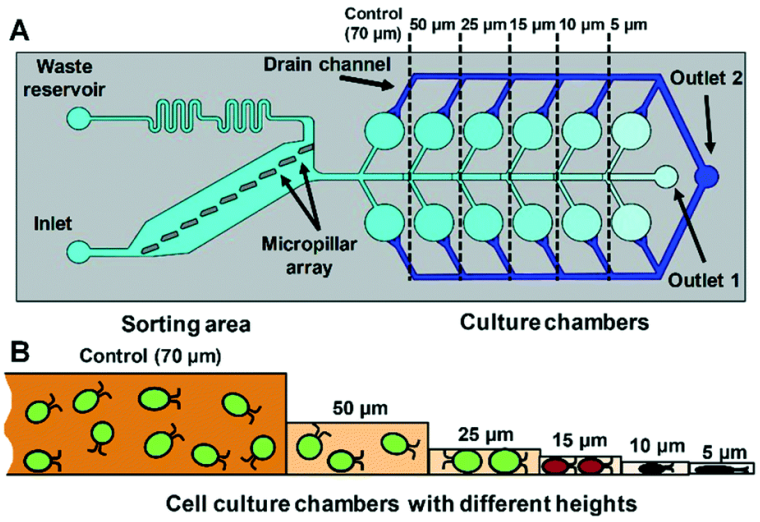


**Figure 2.7** (a) A schematic illustration of the microfluidic *H. pluvialis* culture chip. (b) Cross-sectional view of the culture chambers having six different heights (5, 10, 15, 25, 50, and 70 μm) for different levels of mechanical stress application to cells [62].

Ecological engineering offers a new approach to microalgal biofuel optimization by harnessing interspecific interactions and selecting algal consortia for increased productivity [63]. David N. Carruthers et al. studied interspecific interactions in microfluidic droplets and identified positive associations between different algal species, as well as negative associations [64]. This method allows for high-throughput screening of algal combinations and the identification of productive communities,

leading to more efficient biomass accumulation and bioproduction techniques.

Thijn Verburg et al. explored the use of magnetic artificial cilia to enhance microalgal growth [65]. By introducing motile magnetic artificial cilia into millimeter-scale culture wells, they observed an increase in microalgae density. The hydrophobic surface of the magnetic artificial cilia facilitated the adhesion of microalgae, promoting cluster formation and growth. This approach offers potential for studying the effects of mixing and flow on microalgae and increasing screening throughput.

In summary, novel growth conditions have been investigated to optimize microalgal growth. Controlling intracellular stress levels, exploring multicellular cultures, and utilizing ecological engineering principles offer new avenues for increasing microalgal yield and productivity. These approaches, facilitated by microfluidic technologies, provide researchers with greater control and understanding of the factors influencing microalgal growth, ultimately contributing to the development of more efficient and sustainable bioproduction techniques.

## 2.4 New materials for culturing microalgae: hydrogel in droplets

The use of traditional materials like agar for microfluidic channel manufacturing in microalgae culturing has been replaced by newer approaches. Hydrogel-based systems using agarose gel walls have been developed to provide microalgae with a

constant food supply and protect them from flow shear stress [66]. Beum Jun Kim et al. utilized this hydrogel-based array microhabitat system to examine the growth kinetics of Chlamydomonas reinhardtii over precisely controlled nitrogen gradients [66]. This microfluidic technology offers a faster, more affordable, and quantitative method for studying microalgal growth compared to traditional methods.

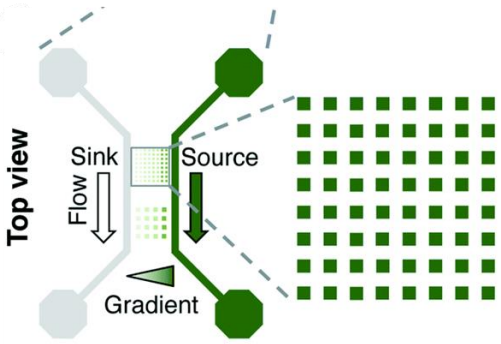


**Figure 2.8** Microfluidic platform design and gradient characterization [66].

Similar approaches have been employed by Brian Nguyen et al., who studied the effects of light intensity and nutrient concentration on microalgal growth using a similar hydrogel-based method [67]. Ming Li et al. demonstrated an inertial microfluidic system that utilizes agar hydrogel droplets to provide nitration to algae [44]. The system allows for the sorting of different-sized hydrogel droplets based on the growth of microalgal colonies inside them [44].

Additionally, Mark van Zee et al. developed the PicoShells hollow shell microparticle

technology, which encapsulates microalgae within 90 μm-diameter particles [68]. These particles have a solid polyethylene glycol (PEG) outer shell and a hollow inner chamber where the cells can grow [68]. PicoShells enable viable downstream recovery, continuous media interchange, phenotypic screenings, and colony compartmentalization [68]. They allow for cell growth in various culture environments and have shown enhanced growth compared to water-in-oil droplet emulsions [68]. These studies highlight the use of hydrogel-based materials, such as agarose gel and PicoShells, in microalgae culturing and screening. These materials provide a controlled and supportive environment for microalgal growth, enabling researchers to study the effects of various factors on microalgal development and optimize culture conditions.

## 2.5 Present limitations

Despite the potential of microalgae, there are several limitations that currently hinder their development and application:

A. Incomplete identification and classification of microalgae species: While there are estimated to be around 70,000 species of microalgae, only a fraction of them have been fully identified and recorded in databases like AlgaeBase. This lack of comprehensive species information limits our understanding of microalgae diversity and their potential applications.

B. Time-consuming droplet generation: Studying new microalgae species or

cultivating large quantities of microalgae often requires the isolation of individual cells. This process is time-consuming and can be challenging, particularly in industrial settings where bacterial and viral contamination is a concern. Generating nutrient droplets with individual microalgal cells can mitigate the risk of contamination but currently involves techniques that are slow and not suitable for high-throughput production.

C. Lack of individual control of large numbers of droplets/cells: Microfluidics offers the advantage of high-throughput screening and monitoring by enabling individual control of droplets or cells. However, as the number of droplets increases, achieving independent control becomes more challenging. The complexity of the microfluidic structure limits the level of autonomy and hinders the full potential of microfluidics in microalgae research and development.

These limitations highlight the need for advancements in species identification, droplet generation techniques, and individual control in microfluidics. Overcoming these challenges will contribute to a deeper understanding of microalgae diversity, more efficient cultivation methods, and improved utilization of microfluidics for screening and optimization.

## 2.6 Future prospects

The future of microfluidics in microalgae research and cultivation holds great

promise for advancing the field and realizing its potential applications. Here are some future prospects:

A. Microfluidic technology for high-throughput analysis and cultivation: Microfluidic devices with high-throughput and high-efficiency capabilities are well-suited for studying microalgae at the single-cell level, separating specific microalgal populations from liquid, and optimizing growth conditions. As advancements are made in microfluidic design and functionality, it is expected that microalgae can be studied and cultivated more effectively, paving the way for applications such as biofuel production and extraction of high-value nutritional supplements.

B. Digital microfluidics for single-cell analysis: Digital microfluidics, which enables the manipulation of individual droplets on an array of electrodes, holds promise for studying microalgae at the single-cell level. Overcoming the challenges of rapid droplet production and achieving high-throughput capabilities will be crucial in the future development of digital microfluidics for microalgae research.

C. Independent control of droplets in high-throughput systems: Current droplet manipulation techniques often struggle to provide independent control of individual droplets in large-scale systems. Finding innovative solutions that preserve the benefits of independent control while reducing the complexity and number of connecting lines will be important for achieving high-throughput droplet

manipulation and expanding the capabilities of microfluidics in microalgae research.

D. Integration of artificial intelligence: The integration of artificial intelligence, big data, and machine learning holds tremendous potential for enhancing our understanding of microalgae and improving algal output. By leveraging AI algorithms to analyze complex datasets and make predictions, researchers can gain deeper insights into microalgae behavior, optimize cultivation conditions, and drive innovation in the field.

Overall, the future prospects of microfluidics in microalgae research involve advancements in device design, droplet manipulation techniques, and the integration of AI for data analysis. These developments will contribute to a better understanding of microalgae, improved cultivation methods, and the realization of microalgae's full potential as a sustainable and valuable resource.

## 2.7 Summary

Microfluidics presents a powerful tool for studying and optimizing the growth conditions of microalgae, which have immense potential as a renewable energy source and a future food supply. Despite the limited number of well-known microalgae species, their versatility and promising applications make them highly valuable. Microfluidic technology offers high throughput, efficiency, and rapidity in observing and differentiating microalgae morphology and improving their growth conditions.

While there are currently limitations and challenges in utilizing microfluidics for single-cell level studies of microalgae, it is believed that digital microfluidics holds promise for advancing microalgae research in microfluidic applications. Further research and development are expected in the use of microfluidics to cultivate microalgae and optimize their growth conditions. Overcoming current limitations and leveraging the potential of digital microfluidics can contribute to the advancement of microalgae research and facilitate their widespread use in various applications.

In conclusion, microfluidics provides a valuable platform for the study and cultivation of microalgae. By harnessing the capabilities of microfluidic technology, researchers can explore the potential of microalgae as a sustainable and versatile resource, ultimately contributing to the development of a more sustainable future.

# Chapter 3 Device Fabrication and Material Selection

The research strategy in this study focuses on utilizing array patterns and microfluidics as the core elements, leveraging their respective capabilities, and advancing microfluidic chip technology to a higher level. The research effort is divided into two main parts: (1) reducing the number of control electrodes required in digital microfluidics, and (2) increasing the quantity (up to 1,000,000 droplet $s^{-1}$) and decreasing the volume (down to pL) of droplets at a faster rate. This chapter will provide an overview of the key chip fabrication methods employed, including photolithography, sputtering, and laser marking. The research team conducted their experiments and fabrication processes at the University Research Facility in Materials Characterization and Device Fabrication (UMF) at Hong Kong Polytechnic University, which houses the necessary equipment for the project.

## 3.1 Brief description of device fabrication

Microfabrication is a critical process in the creation of microfluidic chips, as it involves working with films and scribe lines at the μm level of minuscule characters. Consequently, most of these fabrication activities must be carried out in a cleanroom environment. For the purpose of reducing the number of control electrodes in XY array

chips, which utilize electrodes in multiple orientations on the upper and lower layers in conjunction with DEP concept, the production process involves sputtering. The choice of electrode material also plays a role in the chip's performance. Additionally, the spacing between the electrodes determines the appropriate etching method. The fabrication techniques for two microfluidic chips, which will be discussed in chapters 4 and 5, will be briefly described below.

### 3.1.1Fabrication of XY array chip

The microfluidic device consists of a bottom layer of glass, a plastic spacer (a square-shaped PU plastic with a side length of 6 cm and a thickness of 45 μm) in the middle, and a top layer of glass. Initially, a metal layer is deposited on the bottom and top layers of glass to serve as the base for the electrodes. In order to create insulated electrodes (16 channels), certain areas need to be removed, which can be achieved through laser marking or wet etching. Once the electrodes are produced, the glass is cleaned using acetone, IPA, and DI water in an ultrasonic cleaner for 15 minutes each. A dielectric layer is then formed using materials such as SU-8, $SiO_2$, NOA, or PDMS, depending on the specific requirements. Following that, a hydrophobic layer is coated on the dielectric layer to increase surface tension. The schematic diagram is shown in **Figure 3.1**. Finally, the glass is cut into a smaller size of 6 cm x 8 cm using a laser cutter.

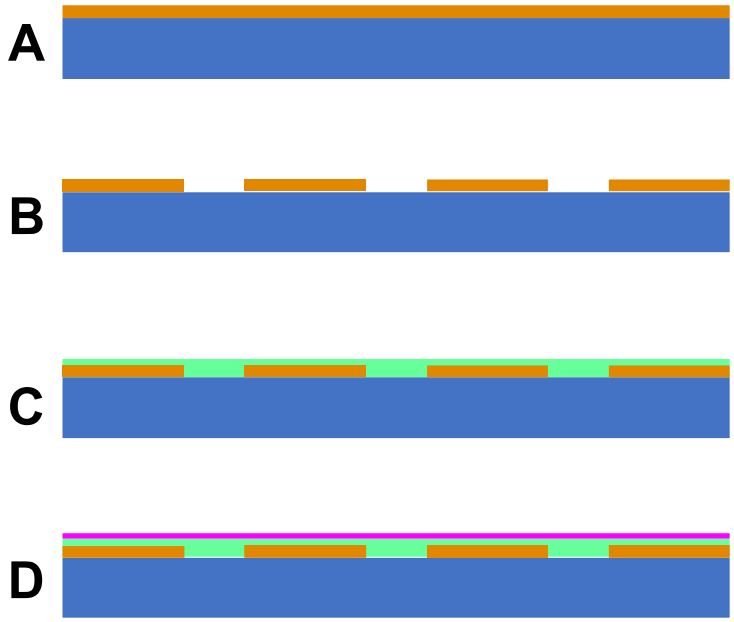


**Figure 3.1** Schematic diagram of the fabrication process for the XY array chip, blue is glass, orange is ITO, green is SU-8 dielectric layer, and purple is land-water layer. (b) Laser-etched ITO glass showing ITO disconnection. (c) Coated with SU-8 dielectric layer for insulation. (d) Teflon coating was applied to increase hydrophobicity.

### 3.1.2 Fabrication of microchip for droplet generation

The microfluidic chip is composed of glass, a metal film, an insulating layer (SU-8 microstructure), and a cover made of PDMS. Initially, sputtering is used to deposit a layer of metal film on a blank glass substrate as a conductive layer. In this case, the metal film thickness can be thicker compared to the previous fabrication step. Subsequently, sputtering is continued to coat an insulating layer on top of the metal layer. Next, an SU-8 microstructure is added on the insulating layer. The schematic

diagram is shown in **Figure 3.2**. Finally, a flat PDMS cover is used to complete the microchip.


**Figure 3.2** Schematic diagram of the fabrication process for the microchip for droplet generation, blue is glass, orange is metal thin film, yellow is insulating layer, green is SU-8 microstructure.

## 3.2 Coating techniques and material selections

The fabrication of microfluidic chips involves careful selection of materials and coating techniques to achieve the desired functionalities. This section provides an overview of key fabrication steps and material selection considerations.

### 3.2.1 Coating techniques

The choice of materials for the conductive layer and electrodes is crucial for the performance of the microfluidic chip. Copper is a cost-effective option with established

coating techniques, but it may be prone to oxidation. Gold is a more sophisticated alternative with better conductivity, but adhesion between gold and glass can be challenging. Indium tin oxide (ITO) is an optimal material for transparent electrodes due to its high light transmission capabilities. The table below compares common materials for electrode fabrication:

**Table 3.1** Comparison of common material for electrode fabrication.

| | **Copper (Cu)** | **Chromium with Gold (Cr/Au)** | **Indium Tin Oxide (ITO)** |
|---|---|---|---|
| **Cost** | $ | $$ | $$$ |
| **Conductive** | $59.6 \times 10^6$ S $m^{-1}$ | $4.10 \times 10^7$ S $m^{-1}$ | $10^4$ S $m^{-1}$ |
| **Coating method** | E-Beam Evaporation, Thermal Evaporation, Sputtering | E-Beam Evaporation, Thermal Evaporation, Sputtering | Sputtering |
| **Transparence** | No | No | Yes |

Three coating technologies will be discussed below: E-Beam Evaporation, Thermal Evaporation, and Sputtering. All three instruments are located within the UMF (PolyU).

*E-Beam Evaporation*

The system's maximum output is 6 K Watt. To begin, regardless of the metal coated, the vacuum must be maintained at 8 x $10^{-7}$ Torr when employing the E-Beam Evaporation technique. The goal of keeping a high vacuum is to reduce the impact of air particles on metal particles during coating. The e-beam was then set to 60 Watts to

guarantee that it hit the target material. For example: 300W for copper will deposit at 6 nm $min^{-1}$, 18W for chrome will deposit at 12 nm $min^{-1}$, and 540W for gold will deposit at Coating at a speed of 6 nm $min^{-1}$. ITO cannot be vapor-deposited since it is not a metal and has a high melting point. **Figure 3.3** shown the E-Beam Evaporation machine used in the thin film coating.


**Figure 3.3** E-Beam Evaporation machine used in the thin film coating.

*Thermal Evaporation*

The system has a 2 K Watt maximum power. No matter what metal is coated while employing the Thermal Evaporation technique for coating, the vacuum level must be

maintained at 5 x $10^{-6}$ Torr. To reduce the impact of air particles on the metal particles during coating, a high vacuum must be maintained. A metal layer is deposited by vapor deposition, which involves vaporizing the metal at a high physical temperature. The heating power is the primary controlling factor during evaporation. Taking the same evaporation rate of 6 nm $min^{-1}$ as an example, the required power for copper, chromium and gold is 260W, 300W and 320W respectively. ITO cannot be evaporated due to its high melting point, similar to e-beam evaporation. **Figure 3.4** shown the thermal evaporation machine used in the thin film coating.


**Figure 3.4** Thermal evaporation machine used in the thin film coating.

*Sputtering*

The two evaporation techniques mentioned above are not the same as sputtering. Sputtering works by using plasma gas stimulation to excite metal particles, which subsequently stick to the target. Since it does not evaporate the target, it is different with evaporation technique. The gas's plasma state was then maintained by adding 30 sccm of argon. Similar to this, a vacuum with an air pressure of $8 \times 10^{-7}$ Torr must initially be maintained when employing the Thermal Evaporation technique for coating, regardless of the metal being coated. Depending on the material to be evaporated, the excited gas can subsequently be put into a plasma state using DC or RF techniques. If the material being evaporated is a metal, DC is typically used due of the quicker speed. Only RF may be utilized if it is non-metal since non-metal does not carry electricity. Here are some correlations between power and deposition speed: Copper was deposited at 60W (DC) at a rate of 7nm $min^{-1}$, Chromium was deposited at 80W (DC) at a rate of 5nm $min^{-1}$, gold was deposited at 80W (DC), The speed is 13nm $min^{-1}$, and ITO is evaporated at 100W (RF), and the speed is 12nm $min^{-1}$. **Figure 3.5** shown the sputtering machine used in the thin film coating.

**Figure 3.5** Sputtering machine used in the thin film coating.

The fundamentals, advantages, and disadvantages of each evaporation process are shown in the table below. Because thermal evaporation and E-beam evaporation have insufficient adhesion forces between the thin film and the substrate, only sputtering was selected as the evaporation method throughout the whole study effort.

**Table 3.2** Comparison of deposition methods for thin film coating.

| | **E-beam evaporation** | **Thermal evaporation** | **Sputtering** |
|---|---|---|---|
| **Theory** | E-beam hits the target, creates a high temperature and generates the gas phase. | To generate the gas phase, the target material is heated using a simple and straightforward physical heating approach. | When plasma-like gas particles collide with the target substance, material particles are produced. |
| **Target material** | Metal with relative low melting point | Metal and semiconductor with relative low melting point | Metal and nonmetal |
| **Initial pressure** | $8 \times 10^{-7}$ Torr | $5 \times 10^{-6}$ Torr | $8 \times 10^{-7}$ Torr |
| **Adhesion to the substrate** | Poor | Poor | Strong |

### 3.2.2 Electrode fabrication

In terms of producing electrodes, it may be separated into positive electrodes and negative electrodes, in addition to modifying PCBs as electrodes. The positive electrode indicates that the substrate is first protected, followed by metal plating, and finally the protective layer and surplus metal are removed. The entire procedure is known as lift off. The negative electrode approach requires that the whole substrate be covered with a metal layer before etching the parts that do not require metal coverage. For negative electrode manufacturing, laser marking and wet etching were employed in this study. **Table 3.3** compares the pros and cons of fabrication methods.

**Table 3.3** Comparison of each method for fabricating electrodes.

| | **Lift-off** | **Wet etching** | **Laser marking** |
|---|---|---|---|
| **Positive or negative method** | Positive | Negative | Negative |
| **Cost** | $$ | $$ | $ |
| **Number of steps** | Photolithography→ thin film coating→ lift off | Thin film coating→ Photolithography→ chemical etching | thin film coating→ leaser marking |
| **Limitation** | The metal film cannot be too thick. | Type of etching solution is limited. Some metal thin film is difficult to etch. | The metal thin film should absorb the laser energy. |

Details on related technology will be provided. The custom-built PCB was not included in this investigation since it is basically constructed of plastic, and plastic flatness is poor. As a result, there may be more or less space in some areas, influencing the droplet movement's stability.

*Lift off*

Lift off is a critical operation in the fabrication of microelectronic devices. The lift off method was used in this investigation at an early stage of the experiment. However, because the space between the electrodes that must be removed is thin and lengthy, the lift off technique was eventually replaced by another procedure.

The substrate is cleaned initially in the early stages of the lift off process, and then the AZ5214E photoresist is spin-coated on the substrate with a spin coater at 500rpm

100RAMP hold 5 s and 4000rpm 500RAMP hold 30 s, and then baked at 105 ℃ for 2 minutes to dry the solvent of photoresists. The baking temperature and time are critical in the creation of a photoresist protective coating. Then place it in the lithography machine and align it with the pre-designed mask before exposing it to the UV l-line dosage of 60mJ $cm^{-2}$. Then, using AZ300MIF developer, remove the exposed photoresist to form exposed regions. Then, using the procedure described in the preceding paragraph, vapor-deposit the conductive layer over it before eventually washing out all of the photoresist with AZ400T remover. In this manner, the conductive layer in the area initially shielded by the photoresist is removed, and the exposed area is covered with a conductive layer, forming electrodes. **Figure 3.6** shown the lithography machine, OAI MBA800 Mask Aligner, used in photolithography.

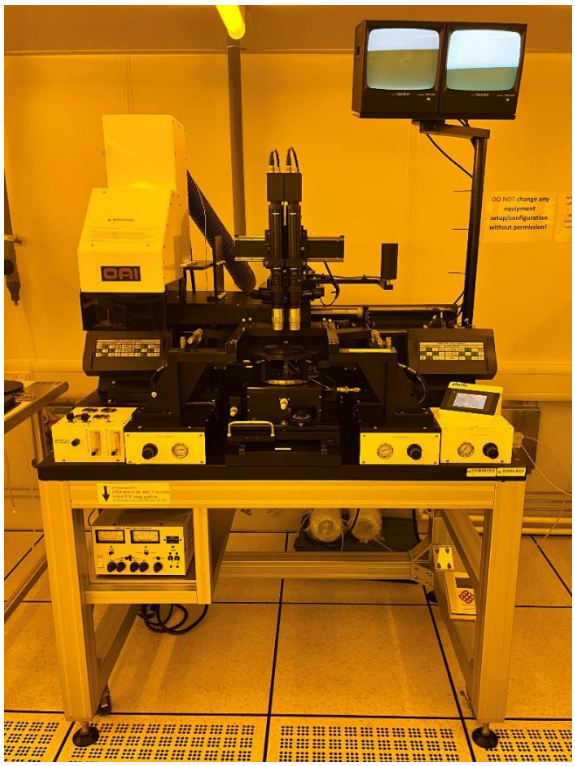


**Figure 3.6** Lithography machine, OAI MBA800 Mask Aligner, used in photolithography.

*Wet etching*

After lift-off, wet etching is the second most prevalent procedure for producing microelectronic devices. Disconnection is common when lengthy and thin lines are required since the lift off procedure involves physical ways to peel off the conducting layer. Wet etching, on the other hand, uses a chemical approach to degrade the conductive layer, avoiding the problem of disconnection. Because the conductive layer in this experiment is mostly ITO, strong hydrochloric acid was utilized for etching. To employ AZ5214E as a protective layer, first evaporate a layer of ITO conductive layer

on the substrate, and then perform the same photolithography method as lift off. The exposed portions of the photoresist are eliminated, much like the lift-off procedure. The duration spent in acid etching was 45 s. But the temperature will affect this parameter. But the mistake is close to 5 s. If the edge is over-etched, a zigzag pattern will develop. Additionally, laser marking, which is used to create electrodes, will soon replace it since it requires concentrated acid.

*Laser marking*

A new wave of production processes is laser marking. Yueming's MF-20-PC is the machine used to carry out the laser marking procedure. Its laser source is a ns pulsed laser with a power of 50W and a wavelength of 1064 nm. He uses a concentrated laser beam to operate on the conductive layer (the diameter of the spot is 40 μm). Due to the fact that the concentrated laser will swiftly convert light energy into heat energy after it contacts the conductive layer, scorching the layer and rendering it non-conductive. The first non-conductive dot is created as a result. To create the next burnt dot, shift the light source a tiny bit. Since most of these two locations will overlap, a burnt line,which represents the region, can then be constructed. A line created by laser burning a conductive layer is seen in **Figure 3.7**. This manufacturing method has also evolved into the primary method for making electrodes in this study strategy since it doesn't require any chemical substances or immersion liquid.

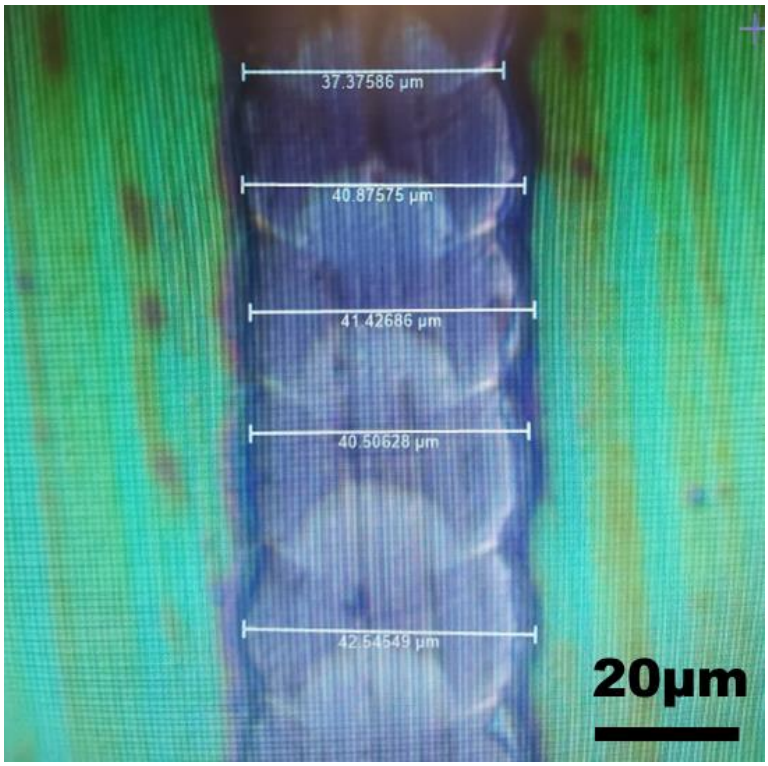


**Figure 3.7** Microscope image of an insulating line formed by laser marking.

### 3.2.3 Materials for dielectric layers

An insulating layer is placed on the conductive layer to prevent electrolysis. This insulating layer should be made of a thin material with a high breakdown voltage and a low dielectric constant. The following table compares the three potential materials. Furthermore, their coating procedures will be introduced one by one.

**Table 3.4** Comparison of electrical properties of insulating layer materials.

| | **$SiO_2$** | **PDMS** | **SU-8** |
|---|---|---|---|
| **Breakdown voltage** | 2700 MV $m^{-1}$ | 635MV $m^{-1}$ | 112 MV $m^{-1}$ |
| **K value** | 4 | 2.3-2.8 | 4.1 |

*$SiO_2$*

Sputtering is a method to sputter $SiO_2$. $SiO_2$ is evaporated at a rate of 3.3 nm $min^{-1}$ at 200W (RF). In general, the coating thickness is around 100nm to prevent the breakdown voltage from being lowered owing to unevenness of the particles during the coating and the thinner sections. Because of its poor coating speed and the frequent occurrence of uneven coating, it is only employed in the early stages of the experiment.

*PDMS*

PDMS has not been widely employed in insulating materials since it is a novel form of polymer. In this research project, it is regarded an insulating layer material due to its ultra-low dielectric coefficient. PDMS is made up of base and citer in a 10:1 ratio. PDMS is still liquid when freshly made, and it may be cured by heating at 65 ℃ for 30 minutes. The thickness of the PDMS film may be controlled by varying the rotation speed and duration to reach the appropriate thickness using the spin coating coating process. If the PDMS layer has to be thinner, add tert-butanol to the liquid PDMS to lower viscosity, and then spin coat to obtain a nanoscale insulating film. **Figure 3.8** shows the relationship between of the thinness of PDMS and speed of spin coating. However, because the PDMS film will expand owing to water absorption, the next substance, SU-8, appears as the insulating layer.

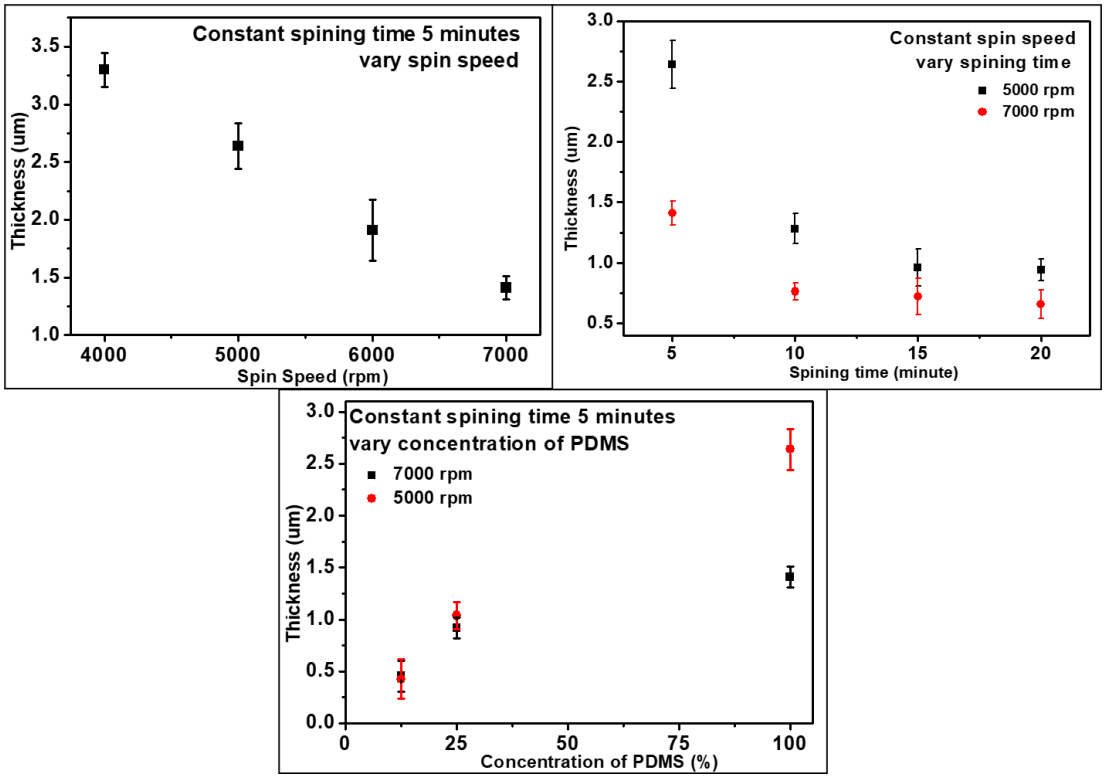


**Figure 3.8** Relationship between of the thinness of PDMS and speed of spin coating.

*SU-8*

SU-8 is a permanent photoresist that has been utilised in the fabrication of microelectronic devices as an insulating layer material. It will also be utilised as a mould in the production of channel microfluidic chips. This time, SU-8 2005 was utilised to create a 5 μm thick insulating layer. First, spin-coat the photoresist on the substrate with SU-8 2005 at 500rpm, RAMP 5 holds 10 s, 3000 rpm, RAMP 10 holds 30 s, then dry the photoresist solvent at 95 ℃. Where insulation protection is required, use 105 mJ $cm^{-2}$ UV l-line. Bake for 3 minutes at 95 ℃ to generate cross connecting where the UV dosage has just been absorbed. Finally, rinse with Propylene glycol

monomethyl ether acetate to remove the photoresist where it does not need to be protected.

### 3.2.4 Materials for hydrophobic layers

Because the contact angle between the droplet and the chip must be increased, covering the final surface with a hydrophobic layer will make the droplet manipulation more visible while also lowering the needed voltage. There are primarily two materials used in evaporating hydrophobic layers: Trichloro (1H,1H,2H,2H-perfluorooctyl) silane (PFOCTS) and Teflon™ AF resin.

*PFOCTS*

Because of its good adherence to the base of the silicon-oxygen connection, PFOCTS was utilized as the material of the hydrophobic layer in the early stages of the experiment. The mechanism transition is seen in **Figure 3.9** when it reacts with the silicon-oxygen bond substrate. It features two coating processes and an atomic film thickness. The first approach involves dissolving 10 mL of PFOCTS in 100mL of water, soaking the substrate in water for 12 hours, then coating the surface with a hydrophobic layer. This approach is pretty straightforward, however it cannot be utilized if the substrate would swell due to water, such as PDMS. The second way is to evaporate it and transfer it to the substrate using a vacuum (low air pressure). Place the substrate in a sealed container first, then add 6-8 mL of PFOCTS, then pump air to -0.9kPa, wait at

least 24 hours before removing the substrate, and a layer of hydrophobic layer can be produced on the substrate. However, Teflon™ AF resin was employed in the middle and later phases of the experiment because PFOCTS can only react with the base of the silicon-oxygen bond to generate a hydrophobic layer and because the thin film of sputtering $SiO_2$ is too thin.

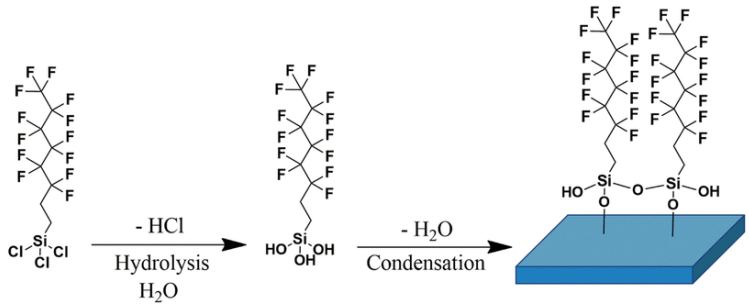


**Figure 3.9** Mechanism transformation diagram of Trichloro(1H,1H,2H,2H-perfluorooctyl)silane (PFOCTS) reacting with silicon-oxygen bond substrate [107].

*Teflon™ AF resin*

The coating process is rather straightforward when Teflon™ AF resin is used as the hydrophobic layer's substance. Start by diluting Teflon™ AF 6200 18% solution with FC40 as a solvent to 1.85, then spin coat the mirror for 30 s at 4000 rpm. After that, bake the mirror for 20 minutes at 65 °C, then dry the FC40 solvent, and bake it for another 20 minutes at 180 °C. Teflon™ AF resin must be baked for at least 20 minutes in order to cross-link. This hydrophobic layer has the benefit of usually always forming

a hydrophobic layer on the surface of any substrate, but it also has the drawback of being easily dissolved by ordinary organic solvents.

The above describes the material selection, key production method, and production process used for microchip fabrication in the project.

# Chapter 4 Microfluidic XY Array for Screening and Culturing of Microalgae

## 4.1 Brief

The use of digital (droplet) microfluidics in the screening and cultivation of microalgae offers great potential for high-throughput sample testing and individual droplet control. This chapter focuses on the development of a digital microfluidics chip with an XY microarray design for microalgae culturing and screening.

The concept of the XY control unit, initially proposed by S.K. Fan in 2003 [67], allows for independent control of individual droplets using a single X+Y connecting wire. While there have been limited studies exploring this concept and its potential applications, researchers have primarily focused on dividing and mixing droplets or controlling one droplet independently on a chip with multiple droplets [68]–[70].

In the context of microalgae screening, where high-throughput testing and sample isolation are crucial, digital microfluidics provides a powerful tool. Alternative approaches, such as fluidic pressure microvalves [71], [72] or laser light guidance [73]–[77], have been explored to manipulate individual droplets. However, these methods have limitations, such as the increased likelihood of failure with a high number of microvalves or the need for a laser light source for precise manipulation.

This chapter presents the utilization of optimized cross-referencing electrode technology for microalgae droplet manipulation in digital microfluidics. Using Euglena as an example, it demonstrates the application of this technique in the screening process for microalgae cultivation. The goal is to showcase the potential of digital microfluidics in the screening and cultivation of microalgae species.

## 4.2 Dielectrophoresis (DEP)

DEP is a label-free particle manipulation technique using an electric field. The force depends on particle and medium dielectric properties [78]–[79]. In a microchannel with integrated electrodes, microalgae experience a non-uniform AC electric field, leading to positive DEP (towards electrodes) or negative DEP (away from electrodes) based on lipid content.

In the theoretical section, as mentioned in Chapter 2.2.2, **Equation (2.1)** clearly illustrates the process of calculating the magnitude of DEP force through particle-environment interactions. In practical applications, reference can be made to **Figure 4.1**, which is divided into three parts: A, B, and C.

**Figure 4.1(a)** demonstrates the scenario where a droplet is exposed to a uniform electric field. In this case, the electric forces acting on the droplet are equal, resulting in no net movement. **Figure 4.1(b)** illustrates a droplet in an electric field closer to the positive pole, causing the electric forces on the droplet to be stronger on the positive side. This

prompts the droplet to move toward the vicinity of the positive pole. **Figure 4.1(c)** further simulates the situation of droplets in an x-connection. Droplets move from the upper and lower grounded electrodes toward the electrodes connected to the power source due to the disparity in electric field strength.

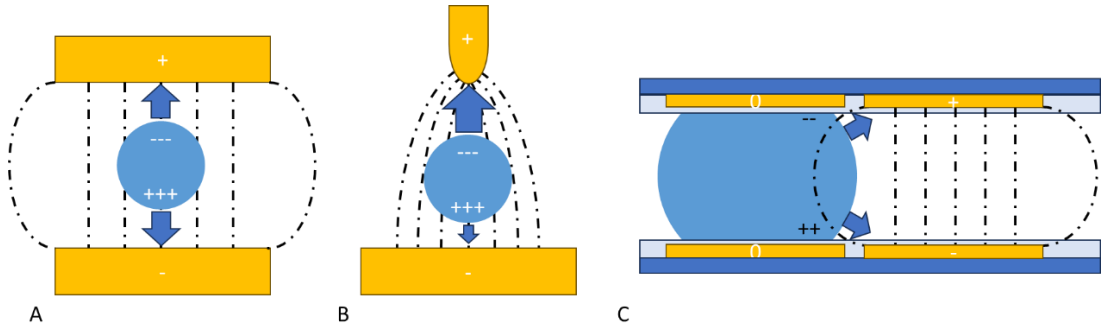


**Figure 4.1** (a) In a uniform electric field, particles experience an equal DEP force. (b) In a non-uniform electric field, particles tend to move towards regions with higher electric field strength in positive DEP case. (c) In the simulation of an XY microarray, droplets are directed towards control units with applied electric fields.

**Equation (2.1)** demonstrates that the DEP force of the dielectric layer's surface is independent of the polarity of the applied voltage. In digital microfluidics, either DC or AC voltages are employed for driving, as the dielectric layer acts as a capacitor and forms a series circuit with the electrode and droplet (**Figure 4.2**).

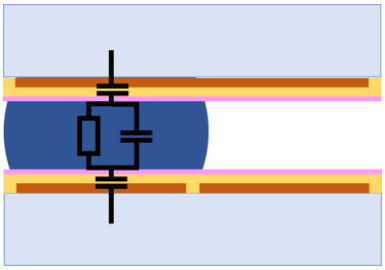

**Figure 4.2** In DEP mode, a simulation of the relationship between the chip and the droplet represented by electronic components.

When a voltage is applied for an extended period, the dielectric layer functions as a capacitor, storing a significant amount of charge and distributing the entire voltage across the series circuit. This limits the working time and makes continuous operation challenging. Applying AC voltage allows the droplet to acquire the same voltage as the electrodes by preventing the dielectric layer from obtaining the full voltage. However, utilizing ultra-high frequency AC voltage poses significant challenges to the circuitry. Therefore, in digital microfluidics using the DEP phenomenon, the frequency of the applied voltage is typically around 1 k Hz [80].

DEP provides a reliable and efficient means of droplet manipulation in digital microfluidics, allowing precise control over the movement and positioning of microalgae droplets on the chip.

## 4.3 Device design and fabrication

*Microfluidic device fabrication*

The whole microfluidic device is formed by a bottom layer glass, a plastic spacer (a square shape 6 cm side length 45 um thick PU plastic) in the middle and a top layer glass. The bottom and top layer glass begin from ITO glass (ITO glass 001 series, <10 ohm $cm^{-2}$ 180 nm thick ITO coating, 10 cm x 10 cm, Kaivo). To create an insulated electrodes (16 channels, @1.8 mm x 7.5 cm), burn off a portion of the ITO coating with a laser etcher (MF-20-PC, 1064nm, ns pulsed laser, 50 W, Yueming). And electrodes were produced. The glass was then cleaned with acetone, IPA and DI water in an ultrasonic cleaner for 15 minutes each solution. A dielectric layer, negative photoresist (SU-8 2010, MicroChem, USA) was spin-coated with a thickness of 10 μm on it. A 200°C post-brake with 20 °C step rise is a must. It protects the layer in the later manufacturing process. After that, to increase the surface tension, a hydrophobic layer has been coated on the dielectric layer. The Telforn solution, 10% of AD-Amorphous Fluoroplastics solution (AF1601 6%, The Chemours Company FC, LLC) with 90% of fluorinert electronic liquid (FC-40, 3M), has been spin coated with 1000 rpm 60 s on it and braked 65 ℃ with 10 minute and 180 ℃ with 20 minute. Finally, the glass was cut to a small size of 6 cm x 8 cm with a laser cutter (532 nm laser source, ZKJ). The difference between the bottom layer and the top layer is that the top layer has 2 inlet holes and 2 outlet holes with a diameter of 1 mm more than the bottom layer. In the operation, the space in the middle of the chip is filled with silicone oil (viscosity of 40

cSt) at the beginning to reduce the control voltage.

*Control equipment setup*

The droplet manipulate is derived from DEP, which requires an electrical signal to provide an electric field difference. The electrical signal comes from a function generator (4011A, B&K Precision). The function generator provides the signal with correct frequency. The signal is then amplified by an amplifier (TDA7498). The amplifier is to provide enough power of the signal. Then it is input to a transformer (6V-220 V with 3 ports at high voltage side). Afterwards, two signals of opposite phases are generated, and they share the same ground terminal. One of the signals uses a digital storage oscilloscope (TBS1154, Tektronix) to monitor their voltage and frequency. Then, they will be connected to multiple relays (JQC-3FF-S-Z, TongLing) to control which electrode is connected to the electrical signal. Each relay can be individually connected to electrical signal or not by controlling. When the electrode is not connected to an electrical signal, it will be grounded by default. Finally, all the terminal lines will be connected into two pin headers (2.54 mm distance) and then connected to the two chips. Scheme diagram as shown in **Figure 4.3**.

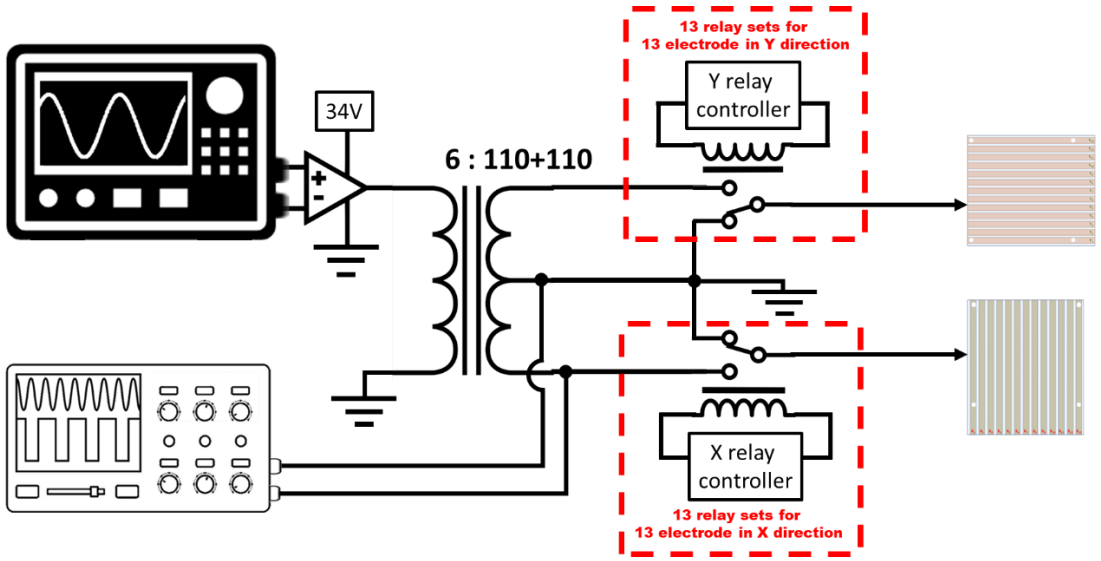


**Figure 4.3** Simulation diagram of circuit resign.

*Device operation*

Because the top electrode glass will be positioned in the X direction and the bottom electrode glass in the Y direction, the top view of the chip will be similar as **Figure 4.4 (a)**. Each "control unit" consists of X-direction electrodes on the top layer and Y-direction electrodes on the bottom layer. In the top left, upper right, lower left, and lower right corners of the controllable area, there will be four access holes. Droplets will enter or leave the chip from these 4 holes. And the cross section image of the chip shown as **Figure 4.4 (b)**.

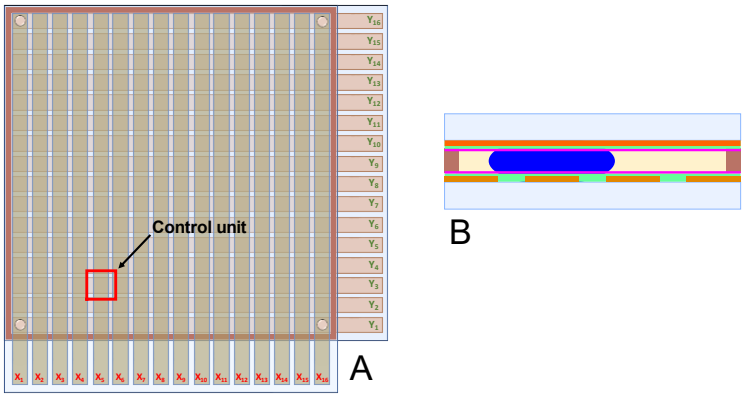


**Figure 4.4** Schematics of the chip (a)Top view of complete chip (b) cross section view.

For the electrical signals, in real operation, it is very similar to the LED display board. If the LED is lit, both the positive and negative side of the LED must be connected to power. Here is an example of how it works in operation.

The (1,1) hole is where the droplet enters. To attract the droplet with the (1,1) control unit, the $X_1$ electrode and the $Y_1$ electrode are activated initially after entry (**Figure 4.5 (a)**), and then both the $X_1$ electrode and the $Y_2$ electrode are energized simultaneously. In this moment, the droplet from the (1,1) control unit will be drawn to the (1,2) control unit by an attractive force (the droplet may stay between the (1,1) control unit and the(1,2) control unit) (**Figure 4.5 (b)**). And then the droplets will be moved to (1,3) by similar method (**Figure 4.5 (c)**). In this step, the minimum drive voltage may to be found, $X_1$ electrode are always active, but $Y_2$ and $Y_3$ electrode are active alternately. And the droplet will be moved between (1,2) and (1,3) back and forth. The drive voltage needs to be adjusted to find the minimum drive voltage.

By analogy, the Y direction electrodes are energized and disconnected one by one, the droplets can be moved from bottom to top to the (1,4) control unit (**Figure 4.5 (d)**) (for an example). Then, by energizing the $X_2$ and $Y_4$ electrodes, the droplet can move from the (1,5) control unit to the (2,4) control unit (**Figure 4.5 (e)**). By analogy, the x-direction electrodes are energized and disconnected one by one, and the droplet can be moved from left to right to the (4,4) control unit (**Figure 4.5 (f)**) (for an example).

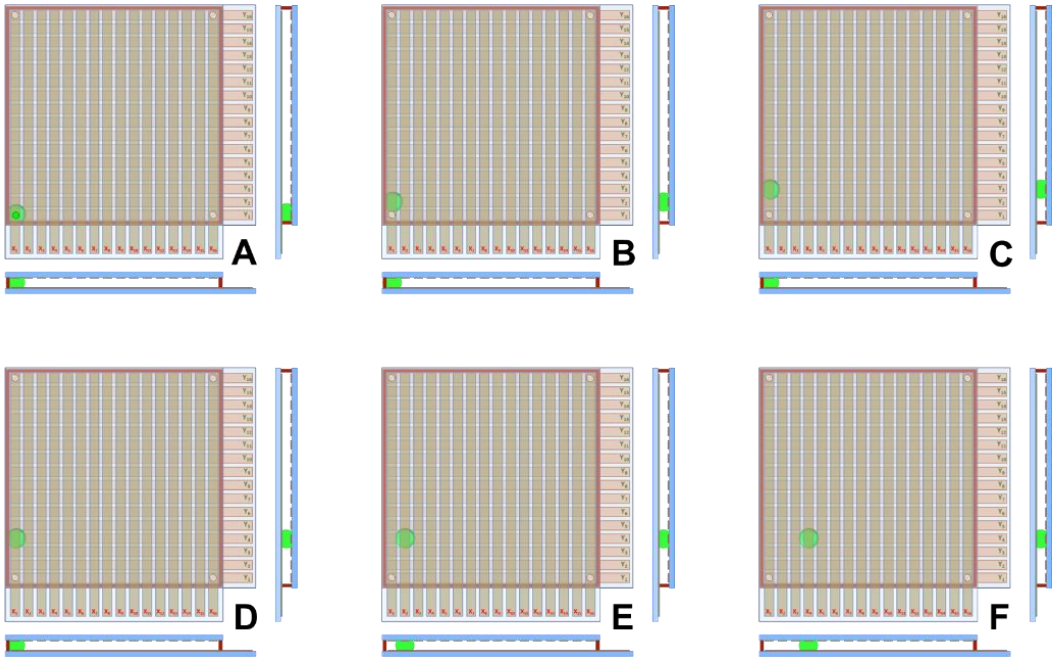


**Figure 4.5** Schematics of the chip: top view and cross section view of droplet moving to each designated control unit.

The same method could be used to transfer more than one droplet to further control units (**Figure 4.6**).

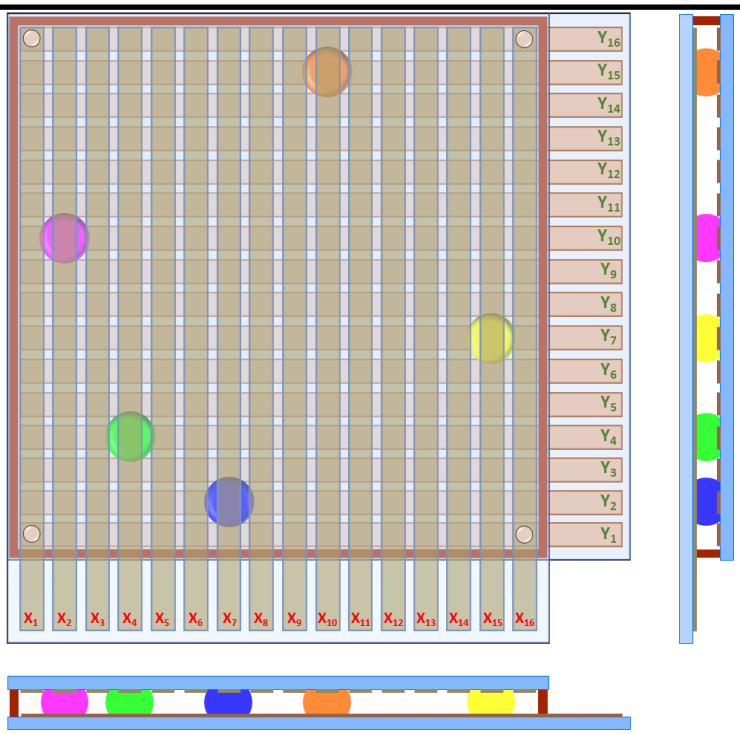


**Figure 4.6 Schematics of the chip**: the top view of each droplet moving to each designated place, and the cross-sectional view in the X and Y directions. This is also the initial position diagram of the droplet.

*Microalgae strains and culture*

The microalgal species in the experiment is *Euglena* (UTEX 753). And the Euglena medium is prepared from UTEX. The medium contains Sodium acetate (Fisher BP 333) 1 g $L^{-1}$, Beef extract Sigma B-4888) 1 g $L^{-1}$, Tryptone (Sigma T 9410)) 2 g $L^{-1}$, Yeast extract (Bacto, Difco) 2 g $L^{-1}$ and $CaCl_2 \cdot 2H_2O$ (Sigma C-3881) 0.01 g $L^{-1}$.

## 4.4 Device operation

**Control**

During the control experiments, the operating voltage was initially set to 300 V as per

device operation specifications. The droplet would move between (1,2) and (1,3) to find the lowest voltage, which may vary due to differences in droplet size, spacing thickness, and movement speed. The minimum applied voltage observed in this experimental setup was 180 V. It should be noted that while multiple droplets can be manipulated on the same chip, only one droplet can be moved at a time during each manipulation movement.

**Speed**

To investigate the relationship between movement speed and drag voltage, a droplet was dragged at a relatively high voltage from the input hole to (4,4), and then it moved along a predetermined path. The voltage was gradually reduced until the droplet became stuck at a certain point. This process was repeated for different speeds, and the minimum applied voltage for each speed was determined. The experiments were conducted three times.

The results showed that when the droplet's movement time from one control unit to another was shorter than 15 ms (corresponding to a moving speed of 0.12 m $s^{-1}$), the required voltage increased rapidly. However, even at the slowest moving speed (the longest movement duration), the voltage did not go below 178V. **Figure 4.7** illustrates the relationship between the minimum applied voltage and the droplet's speed, indicating that the speed has a positive relationship with the square of the applied

voltage.

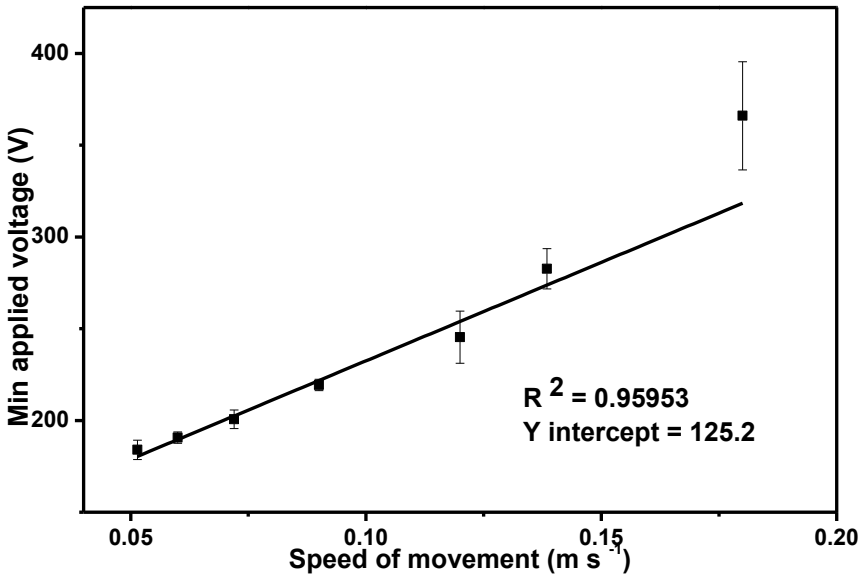


**Figure 4.7** Graph of minimum applied voltage versus speed of droplet movement.

**Microalgae droplet movement**

Similar to the control experiments, the movement of droplets containing microalgae and nutrient solution was tested. The droplets followed the same path as in the control experiments but contained a nutritional solution with microalgae. The results showed that the microalgae droplets could move through the chip and circuit design without interfering with each other, confirming the successful transfer of microalgae to the desired areas on the chip.

These results demonstrate the effectiveness of the digital microfluidics chip with XY microarray for manipulating droplets and specifically moving microalgae droplets in a

controlled manner without affecting other droplets.

**Real microalgae applications**

The nutrient solution containing microalgae was placed within a microfluidic chip for screening and cultivation purposes. As illustrated in **Figure 4.8**, at the initial stage on day 0, the microalgae count in the droplet was 1.

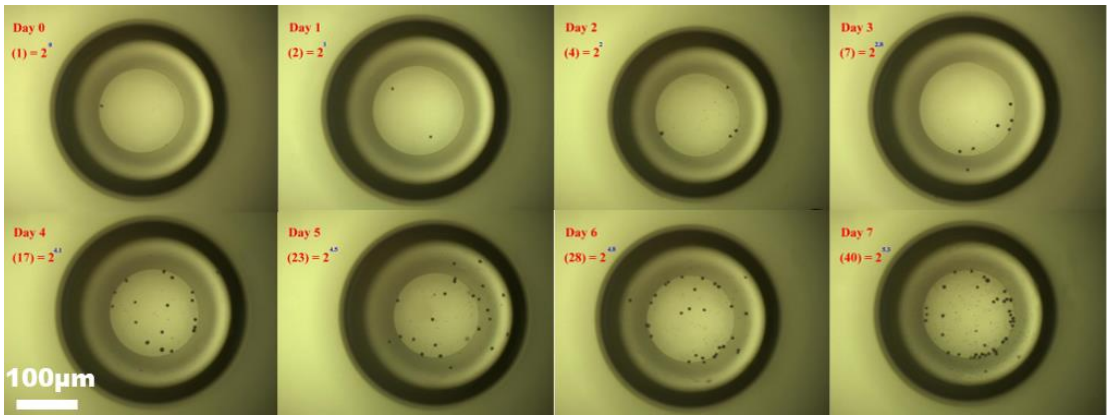


**Figure 4.8** Photo of microalgae in a single droplet.

Over time, there was a continuous proliferation of microalgae in the droplet, reaching 40 on day 7, equivalent to $2^{5.3}$. Detailed daily growth patterns are provided in **Table 4.1**. The chart presents a comprehensive depiction of the nuanced variations in microalgae quantities over the specified time period. This experiment aims to explore the proliferation dynamics of microalgae at different time points, providing valuable insights into their growth mechanisms.

**Table 4.1** Proliferation dynamics of microalgae in a single droplet

| **Day** | **0** | **1** | **2** | **3** | **4** | **5** | **6** | **7** |
|---|---|---|---|---|---|---|---|---|
| **Microalgae count** | 1 | 2 | 4 | 7 | 17 | 23 | 28 | 40 |
| **$Log_2$** | 0 | 1 | 2 | 2.8 | 4.1 | 4.5 | 4.8 | 5.3 |

Furthermore, in addition to independently manipulating regular droplets, dedicated control experiments were conducted on droplets containing microalgae and those devoid of microalgae. The outcomes, as illustrated in **Figure 4.9**, demonstrate that even when the microalgae-containing droplet moves adjacent to a non-target droplet, the non-target droplet remains impervious to interference. This substantiates the capability of the designed system for microalgae screening and individualized manipulation.


**Figure 4.9** Photo of independent manipulating with microalgae-containing droplet

## 4.5 Experimental results

**Individual control with threshold voltage**

The control equipment configuration separates the electrical signal into in-phase and out-of-phase components. This results in different phases for the electrodes on both

sides of a control unit. For example, in the (5,5) control unit, the electrodes on both sides are in entirely different phases, leading to a higher-than-threshold voltage and successful DEP driving force. However, control units that utilize only the X5 or Y5 electrode have only half of the electric field and attractive force, as only one side of the electrode is energized while the other side is grounded.

When both the X5 and Y5 electrodes are activated, the (5,5) control unit generates enough attractive force to move droplets from all nearby control units to (5,5). However, other control units that use either the $X_5$ or $Y_5$ electrode alone generate only half of the attractive force, which is insufficient to attract droplets from nearby control units. This limitation is illustrated in **Figure 4.10**.

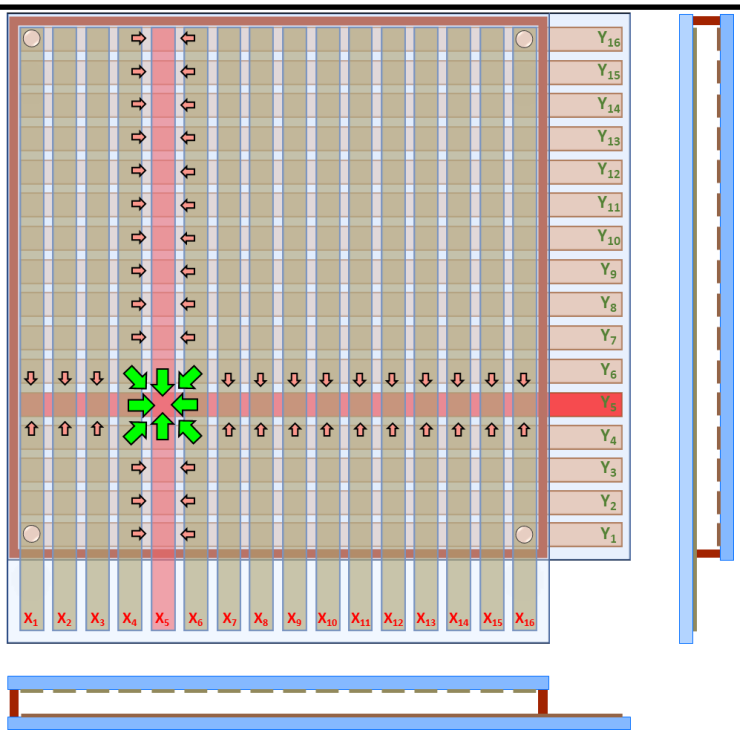


**Figure 4.10** By applying electrodes on $X_5$ and $Y_5$ electrode, the droplet surrounding the control unit (5, 5) will have enough force to move to (5, 5). But other droplets on the edge of $X_5$ and $Y_5$ electrode failed to move to $X_5$ electrode and $Y_5$ electrode.

The threshold voltage plays a crucial role in the control of droplets using the DEP effect. The applied voltage must exceed the threshold voltage for droplet movement to occur. However, the voltage displayed by the measurement equipment is only half of the threshold voltage since one electrode receives the voltage while the other electrode is in the opposite phase. Therefore, the control unit receives twice the potential difference displayed by the measurement equipment, which corresponds to the threshold voltage. It is important to note that the applied voltage should not exceed twice the lowest applied voltage in this approach.

If the applied voltage exceeds twice the threshold voltage, all control units that have one electrode applied with voltage and the other electrode grounded will experience a voltage higher than the threshold voltage. This leads to the droplets near those control units being attracted to the wrong control units, hindering the independent movement of individual droplets. Therefore, it is most effective to apply a voltage slightly above the threshold voltage to avoid unwanted droplet movement and interference.

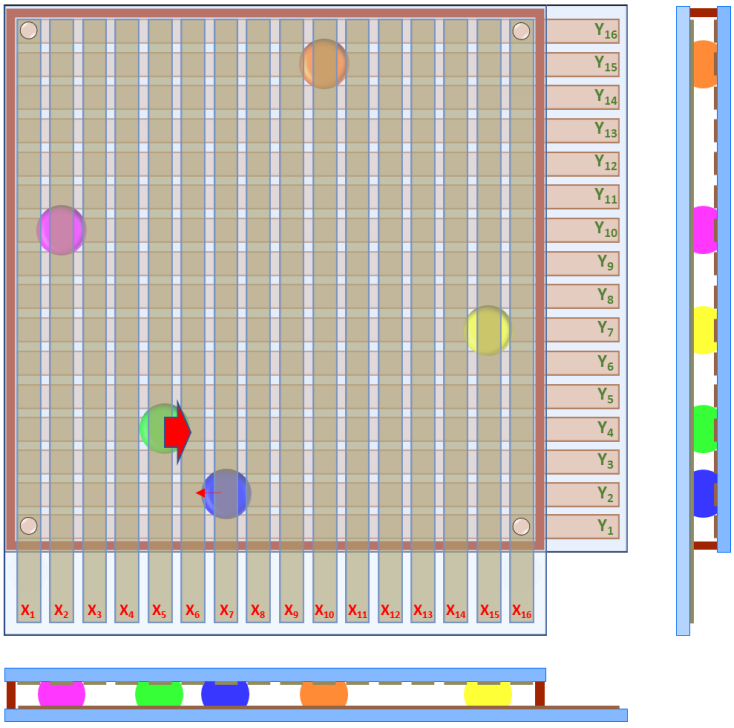


**Figure 4.11** When the $X_6$ and $Y_4$ electrodes are applied, the droplet at (5, 4) has sufficient force to move to (6, 4), but the droplet at (7, 2) does not have enough energy to move to (6, 2).

**Moving speed vs voltage**

As stated in the previous chapter, when the applied voltage exceeds the threshold voltage, the droplet moves. This is because the DEP force adding to the droplet parallel to the plate, and make the droplet make to the control unit applied electrical power. The more voltage applied, the greater the change in contact angle and the faster the droplet movement. As a result, when the speed of the droplet movement is considered, the minimum voltage required increases when the droplet is required to move at the fastest speed. This voltage should be proportionate to the rate of movement. **Equation (2.1)** shown the relationship between electrical field and DEP force.

$$F = ma \ = m\frac{v}{t} = \pi \, \varepsilon_m \ a^3 \, Re \left[\frac{\tilde{\varepsilon}_p - \tilde{\varepsilon}_m}{\tilde{\varepsilon}_p + 2\,\tilde{\varepsilon}_m}\right] \nabla \, |E|^2 \qquad (4.1)$$

**Equation (4.1)** is simplified to provide the following relationship:

$$\frac{v}{t} = \frac{d}{t^2} \propto V_{app}^2 \qquad (4.2)$$

We may verify that the experimental findings are compatible with the formula's inference by calculating the relationship between the moving speed and the applied voltage in the real driving outcomes, and it has been shown as **Figure 4.10**. The Y intercept of the relationship shown the minimum applied voltage is 162V by calculation.

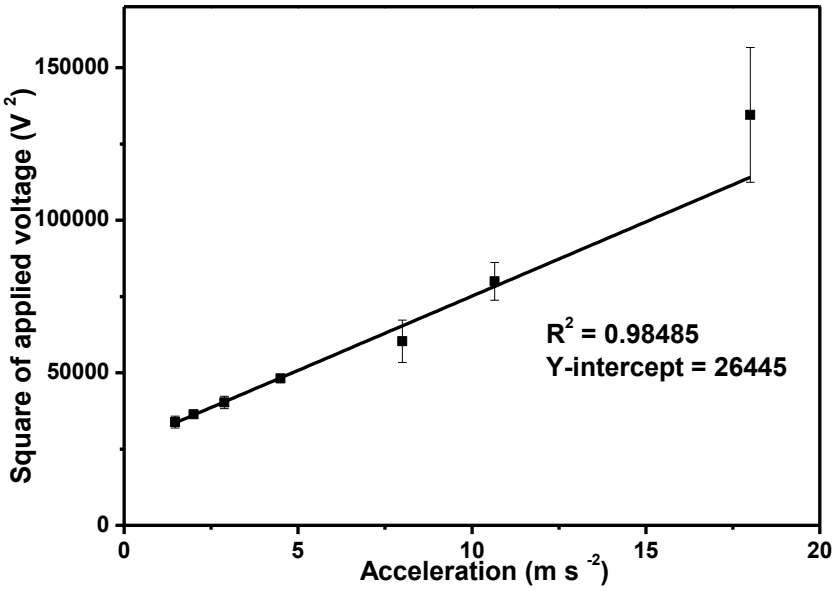


**Figure 4.12** Graph of square of minimum applied voltage versus acceleration of droplet movement.

Furthermore, the dose of strong electric field absorbed by the droplet should be minimized as much as feasible during movement. This dosage may be expressed as follows:

$$E = Pt \qquad (4.5)$$

Among them, power (P) can be defined as:

$$P = \frac{V^2}{R} \qquad (4.6)$$

So,

$$E = \frac{V^2 t}{R} \qquad (4.7)$$

Because R is constant, the droplet's high electric field dosage may be simply interpreted as the product of "$V^2$ t." However, **Equation (4.7)** shows that V and t have an inverse

connection. Because, in order to limit the dose of strong electric field absorbed by the droplet, it should be dropped to get the lowest electric field (longest droplet travel time) with the lowest driving voltage. This reduces the amount of intense electric field dosage absorbed by the droplets.

**Microalgae application**

Because this design combines the benefits of XY arrays with droplet digital microfluidics, several samples may be processed on the same small chip at the same time. Humans have a firm grasp of 50,000 microalgae species, while biologists believe that there are up to 1 million microalgae species in the globe. [26] Species of algae As a result, the application context of this paper is microalgae applications.

Same as the original experiment, the identical process was repeated, but this time all droplets were replaced with droplets containing abundant microalgae, the droplets in question all traveled and remained in their intended locations.

However, since the droplet must apply a voltage in order to form a strong electric field, and this strong electric field may have an influence on biological cells, including whether the strong electric field affects the activity of live cells and if the joule heat effect heats the liquid.

Concerning whether cells attracted by a high electric field will become inactive or have lower activity, we did another experiment to demonstrate that the microalgae treated

with a strong electric field had no significant influence on activity. Apply a 236 $V_{rms}$ (e-field = 4M V $m^{-1}$), 2k Hz AC signal to a nutritional solution containing *Euglena* (500 x $10^3$ cells per mL) for 3 minutes, which is longer than a normal operation time for serval times. As illustrated in **Figure 4.11**, the total period for each application of the electric field should not exceed 30 s from the time the droplet enters the chip to the time it departs the chip. The liquid was then placed in a room with light, and a nutritional solution (including *Euglena* cells) was utilized as a control experiment under the same conditions but not drawn by the strong electric field. The higher quantity of microalgae in the nutrient solution, the lower light transmittance, and the visible light absorption peak of *Euglena* is approximately 675nm. [81], [82] After 2 weeks, the absorption peak (non-fluorescence) at 675 nm of the nutrient solution containing microalgae was tested by UV-Vis spectrometer (Brand: SHIMADZU), and both were significantly increased compared to the samples at the start of the experiment, indicating that they all reproduce by cell division after 2 weeks inside. However, there is no statistically significant change in the results between the two, proving that *Euglena* cells were not decreased or inactivated by applying a high electric field. As illustrated in **Figure 4.12**.

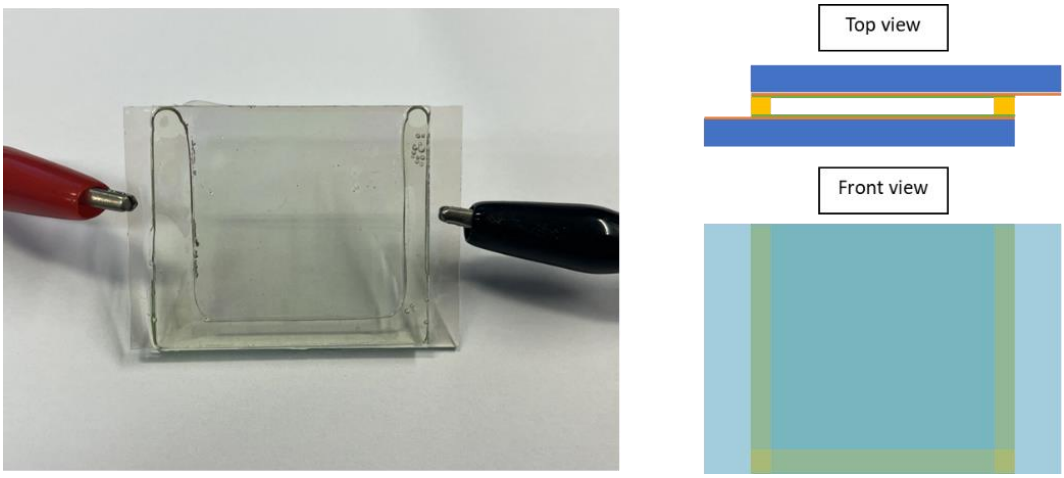


**Figure 4.13** Experimental design to apple strong electric field to the solution, and the simulation of top and front views of the chip.

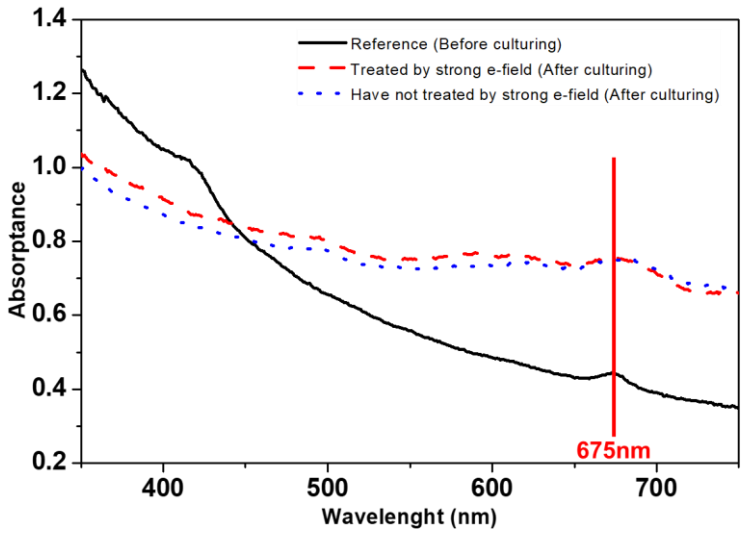


**Figure 4.14** The absorptance of each microalgae sample in the visible light band. The solid line is the sample that has not started the experiment as a reference, the red long dashed line is the sample that has been treated with strong electric field and cultivated for 2 weeks, and the short blue dashed line is the sample that has not been treated with strong electric field and cultivated for 2 weeks.

We also performed an additional experiment that was more severe than the actual circumstance to demonstrate that the joule heat effect had little influence on chip function. As illustrated in **Figure 4.13 (a)**, the prior experiment to determine cell viability was performed, but this time in a thermally insulated environment. Simultaneously, the time required to apply the electric field has been increased from 3 minutes to 30 minutes, ensuring that if the application of the electric field causes the chip of this design to heat up, the heat energy may be detected. As illustrated in **Figure 4.13 (b) and (c)**, the temperature of the chip (containing the water droplets) rose from 26 ℃ to 30 ℃ (the ambient temperature was 24 ℃). Because the error of an infrared thermal imager (Brand: FLIR, Model: E8-XT WiFi), to monitor temperature, is 2 ℃, as a result, the chip's temperature rise may be mostly disregarded.

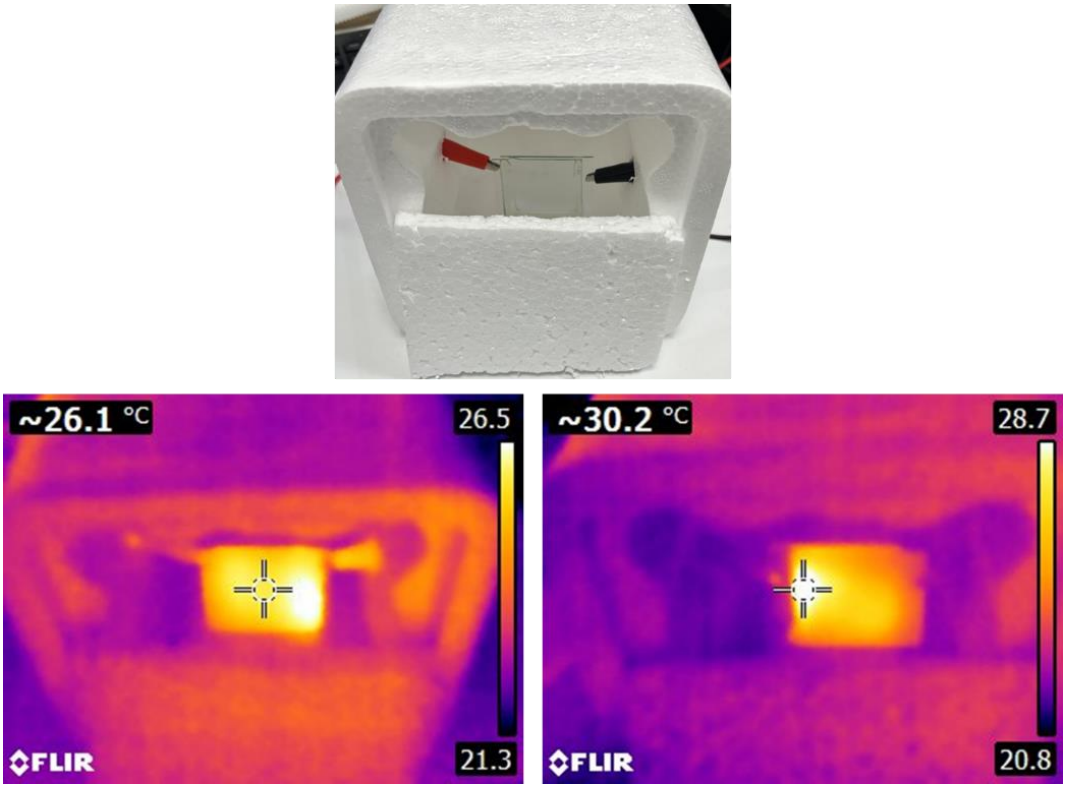


**Figure 4.15** (a)Experimental design in an insulated environment. (b) The chip temperature was 26.1 ℃ before the start of the experiment. (c) At the end of the experiment, the hottest part of the chip was 30.2 ℃.

## 4.6 Discussions

The future applications of the digital microfluidics chip with XY microarray technology extend beyond the screening of microalgae species. While microalgae screening remains a significant application due to the vast number of unidentified species, the versatility of this technology opens doors for various other applications.

One potential application is in cancer medication screening. With the ability to control

thousands of droplets independently on the same chip, each droplet sample can be exposed to different combinations of medications, allowing for efficient and high-throughput screening of potential cancer treatments. This technology could accelerate the discovery and development of effective drugs for cancer therapy.

Another application lies in the identification of harmful compounds at border crossings. By integrating the digital microfluidics chip with XY microarray into a portable and automated system, samples collected at border checkpoints can be quickly analyzed for the presence of dangerous substances. This can aid in detecting illicit drugs, hazardous chemicals, or other prohibited materials, enhancing security measures.

The large-scale polymerase chain reaction (PCR) screening of infectious diseases is another potential future application. The chip's capability to handle numerous droplets simultaneously enables efficient screening of a large number of samples for the presence of specific pathogens. This can significantly expedite the diagnosis and surveillance of infectious diseases, contributing to timely interventions and control measures.

In addition to these advanced applications, the technology holds promise for educational purposes, including middle school science studies. The user-friendly nature and potential miniaturization of the digital microfluidics chip make it a valuable tool for introducing students to the field of microfluidics and molecular biology. Students

can perform hands-on experiments and gain practical insights into fluid manipulation and biological analysis, fostering their interest and understanding of scientific concepts. Overall, the digital microfluidics chip with XY microarray technology has a wide range of potential applications beyond microalgae screening. Its ability to independently control multiple droplets on a single chip opens up possibilities for various fields, including cancer research, security screening, infectious disease diagnostics, and science education. Continued research and development in this area will further enhance its capabilities and impact in diverse applications.

## 4.7 Summary

The digital microfluidics chip with XY microarray technology demonstrates its potential for various applications, including microalgae screening, cancer medication screening, compound identification, infectious disease diagnostics, and science education. Its ability to independently control multiple droplets on a single chip enables high-throughput sample testing and analysis. Further research and development in this field hold promising prospects for advancing these applications and driving innovation in screening, diagnostics, and education.

# Chapter 5 EWOD Templated Pressing Method for Generation of Large Arrays of Picoliter Droplets

## 5.1 Brief

A fundamental distinction between digital microfluidics and conventional microfluidics lies in the treatment of each droplet as a separate entity. This unique characteristic emphasizes the importance of rapidly manufacturing droplets of consistent size and shape in digital microfluidic systems.

The formation of droplets requires the presence of two immiscible phases. The relationship between the medium and the droplet is relative, wherein the dominant liquid becomes the medium and the other liquid becomes a component of the droplet. The selection of the medium and the liquid phase within the channel determines whether the droplets are generated by the continuous phase or the dispersed phase. Key factors such as the interfacial tension between the droplet and the medium, the flow rate ratio, and the channel geometry influence the size of the produced droplets.

Microdroplet generation techniques can be categorized into two types: passive and active. Active techniques involve the application of external energy, such as electrical

energy, magnetic force, or centrifugal force. However, active methods often result in lower droplet size homogeneity. Passive microdroplet generation techniques, on the other hand, encompass various channel designs including cross flow, flow focusing, and cooperative flow, yielding droplets with improved size uniformity.

In this chapter, we will explore several methods for droplet creation, including DEP-driven droplet generation, liquid-liquid micropatterns, and liquid injection (T-Junction).

*DEP-driven droplet generation* [83]

This technique involves applying a voltage above and below a non-polar liquid, causing the droplets to be drawn in and expelled due to the resistance of the liquid. It differs from EWOD method described earlier. DEP-driven droplet generation can produce droplets as small as 10 pL.

*Liquid–Liquid Micropatterns* [84]

By treating specific areas of the surface with hydrophilic and hydrophobic properties, changes in surface tension occur, enabling the generation of droplets. This method offers high-speed droplet production, with the capability of generating 1000 droplets in less than 10 s. However, it is limited to droplet diameters of 1 mm due to the air-based process.

*Liquid injection (T-Junction)* [21]–[23]

In this technique, the primary flow channels are formed by the two sides of the T-shaped structure, while the liquid that generates the droplets enters the main channel through the third channel. The flow rate ratio plays a crucial role in droplet formation. Incorrect flow rate ratios can affect droplet size, and if the ratio approaches unity, a stratified flow may occur. By intentionally narrowing the droplet liquid channel at the T-junction, smaller droplets can be generated.

To compare these droplet generation processes, refer to **Table 5.1**.

**Table 5.1** Comparison of common droplet generation processes.

| | **Liquid–Liquid Micropatterns** [84] | **Liquid injection** [21]–[23] | **DEP-driven droplet generation** [83] |
|---|---|---|---|
| **Active or passive** | Passive | Passive | Active |
| **Time for generating 1000 droplets** | Short (<10 s) | Long (~ 16min) * | Very long (~ 1 h) |
| **Volume of smallest droplet** | 1mm | 240um ~7.5nl | 12.4um 10 pl |
| **Remark** | | The most common method in microfluidics | |

The ability to generate droplets at the pL scale enhances the advantages of microfluidics, as it further minimizes sample volumes. In conventional methods, producing pL-level droplets is challenging due to surface tension limitations. However, in the following

section, we will present a technique that overcomes this constraint and enables the creation of droplets with volumes as small as 0.9 pL.

## 5.2 Surface tension

The high surface tension of water poses a challenge in the production of small droplets using conventional methods, preventing droplets from reaching the pL scale. This section explores the difficulties associated with creating small droplets when the liquid exhibits high surface tension.

In cohesive liquids, such as water, the molecules strive to minimize the surface area, resulting in droplets merging upon contact. The cohesive force generated by a droplet is a manifestation of its surface tension, which aims to reduce surface potential energy. At the molecular level, in a perfectly spherical droplet, the molecules are pulled towards the center by neighboring molecules in all directions, resulting in a balanced molecular force (as depicted in **Figure 5.1(a)**). However, during droplet formation, when a smaller droplet separates from a larger droplet, there is an unbalanced gravitational force at the point of separation (as shown in **Figure 5.1(b)**). This causes molecules at the surface to be drawn inward, reducing the surface area and giving rise to surface tension.

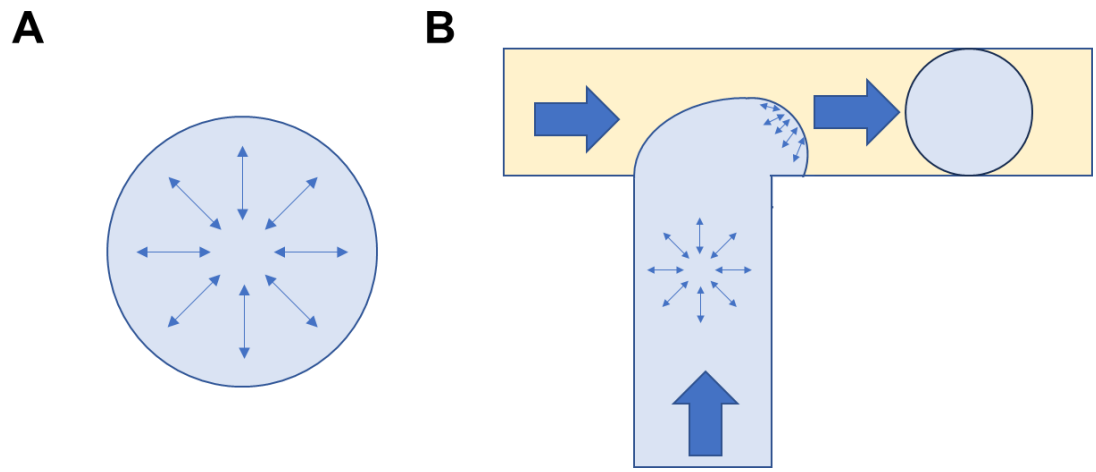


**Figure 5.1** Molecular forces in liquid (a) droplet in sphere (b) at the moment of generating droplet in T-junction.

Naturally formed droplets exhibit a minimum volume directly proportional to their surface tension. The measurement of surface tension can be carried out using the drop weight method, based on Tate's Law. Tate's Law states that the surface tension ($\boldsymbol{\gamma}$) of a droplet can be calculated using the following equation:

$$2\,\pi\,r\,\gamma = m\,g \tag{5.1}$$

where $r$ is the droplet's radius, $m$ is its mass, and $g$ is the acceleration due to gravity.

Rearranging Tate's Law to solve for $r$ yields:

$$r = \frac{m\,g}{2\,\pi\,\gamma} \tag{5.2}$$

Considering the mass of a droplet in terms of its volume (V) and density ($\boldsymbol{\rho}$), the equation becomes:

$$r = \frac{V\,\rho\,g}{2\,\pi\,\gamma} = \frac{2\,r^3\,\rho\,g}{3\,\gamma} \tag{5.3}$$

Hence, the relationship between droplet size, liquid surface tension, and density can be expressed as:

$$r = \left(\frac{3\,\gamma}{2\,\rho\,g}\right)^{\frac{1}{2}} \tag{5.4}$$

According to **Equation (5.4)**, under specific conditions, such as density and other variables, higher surface tension leads to the formation of larger droplets naturally, resulting in larger droplet radii.

Water has a surface tension value of approximately 72.75 mN $m^{-1}$, which is relatively high. Consequently, the spontaneous creation of pL-sized droplets is challenging, as the mutual impact of droplets can easily cause them to merge and form larger droplets.

Forming liquid droplets in a high surface tension liquid without being influenced by the high surface tension is precisely the challenging issue. In the following sections, a structure will be described that utilizes pores within a microstructure to introduce liquid into the pores and subsequently expel the liquid outside the pores. The key technology for the entire device lies in the method of introducing liquid into the pores.

## 5.3 Experimental method

*Microfluidic device fabrication*

The fabrication of the droplet generation device involves the use of a substrate with a conductive layer, an insulating layer, and a micropattern layer. In the experiment, glass

is chosen as the substrate for ease of processing, while ITO (Indium Tin Oxide) is selected as the material for the conductive layer. A 100 nm thick layer of ITO is coated on the glass substrate using sputtering. An insulating layer of 10 nm $SiO_2$ is then applied on top of the conductive layer. Lastly, a micropattern layer is created by spin-coating a negative photoresist (SU-8 2005, MicroChem, USA) with a thickness of 4 μm. A conductive wire is connected at the corner of the chip to allow for voltage application and removal of air bubbles inside the micropattern.

*Device operation*

To begin the device operation, a wire is carefully placed into a deposited droplet on the chip, ensuring that it does not touch the microstructure layer to avoid any damage. A direct current is then applied to the conductive layer and droplet. The voltage starts at zero and gradually increases until a decrease in the liquid's contact angle is observed. Usually, the voltage is 10-20 V, depends on the size of well. Simultaneously, bubbles will form within the droplet, indicating the release of air that was trapped within the microstructure layer. The wire can be removed, and a PDMS (Polydimethylsiloxane) layer, which has been cured as a flat surface on a Si wafer, is applied to remove any excess liquid. Due to the thinness of the liquid layer (4 μm), a methylene blue solution is used in the experiment, as its deep blue color can still be easily detected under a microscope.

By following this experimental method, the droplet generation device can be effectively operated and the generation of small droplets can be observed and analyzed.

## 5.4 Experimental results

**Micropattern**

The microstructure layer was successfully created using SU-8 2005 photoresist, as shown in **Figure 5.2**. The microstructure layer consisted of μm-sized pores, with the central aperture acting as the "well" for droplet formation. The size of the "well" determined the volume of the droplet.

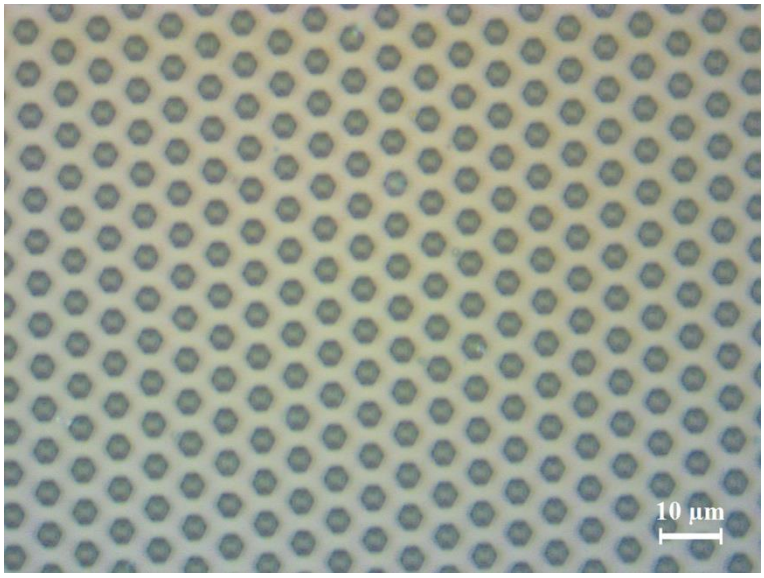


**Figure 5.2** Microscope image of the microstructure layer fabricated with SU-8 photoresist.

**Microdroplet generation**

**Figure** 5.3 illustrates the microscope images of the PDMS module with the microstructure layer. In **Figure** 5.3(a), which represents the device without voltage applied, the "wells" appeared empty. In **Figure**s 5.3(b) and (c), where the methylene blue solution was added, the presence of the solution was observed. **Figure** 5.3(b) shows the result without applying voltage before covering the "wells" with PDMS, while **Figure** 5.3(c) shows the result with voltage applied. The application of voltage led to the presence of the methylene blue solution in almost all the "wells" on the chip after PDMS covering.

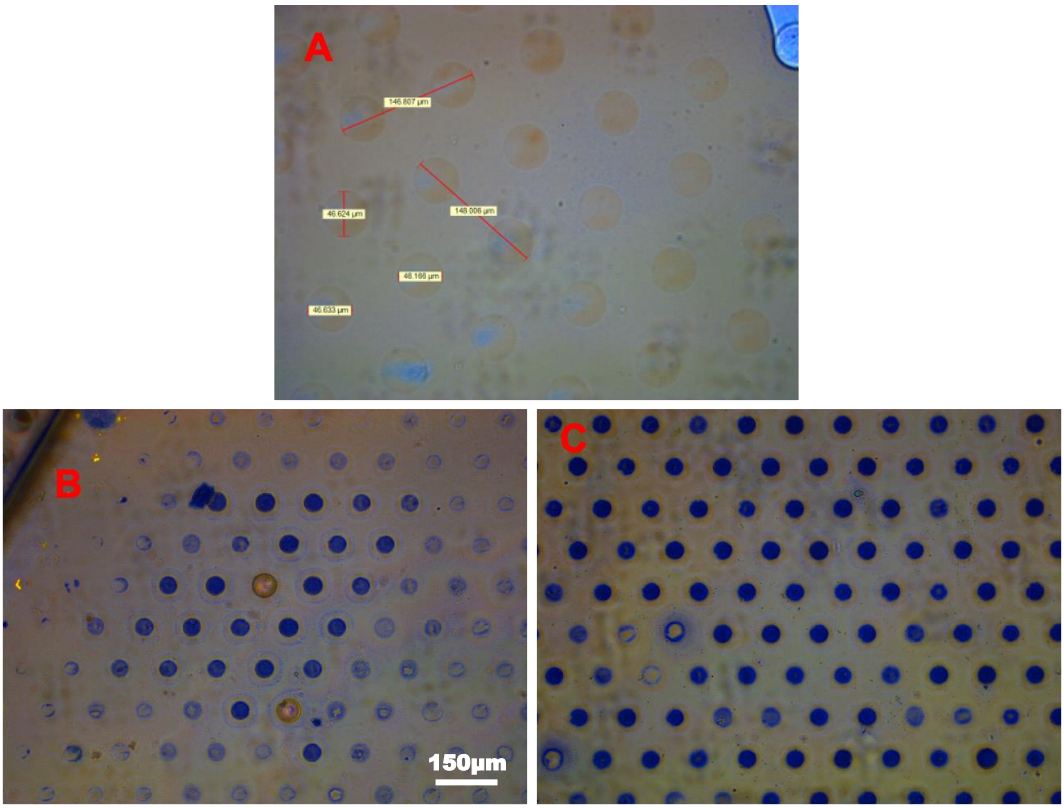


**Figure 5.3** Microscopic image of the PDMS module with Si wafer as the curing mold on the microstructure layer. (a) Cover PDMS directly without adding any liquid. (b) and (c) are images of PDMS after adding methylene blue solution. (b) No voltage was applied before capping; (c) 15 V was applied before capping.

During the experiment, a microstructured layer with a pore size of 17 μm and a depth of 4 μm successfully produced microdroplets with a volume of 0.9 pL, as depicted in **Figure** 5.4.

These results demonstrate the successful generation of small droplets using the developed microstructure layer and experimental setup. The droplets can be precisely

controlled and their volume can be tailored by adjusting the pore size and depth of the microstructure layer.

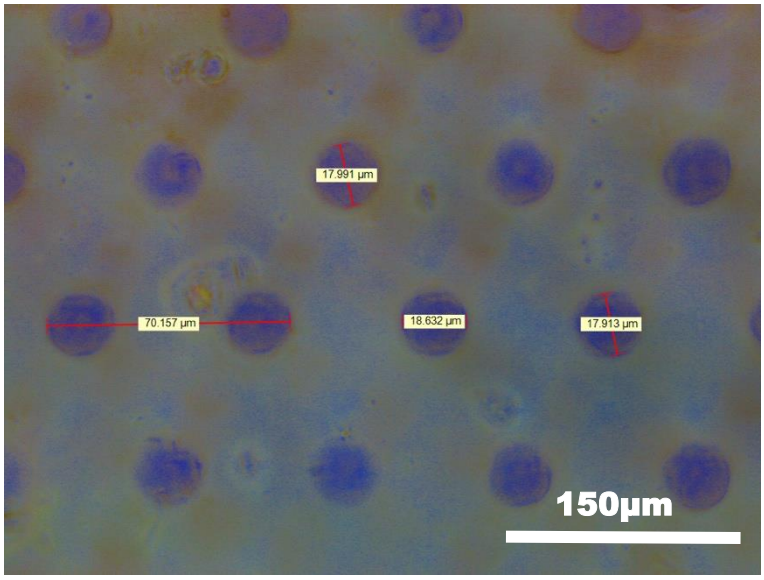


**Figure 5.4** Microscope image of a droplet volume of 0.9 pL. The pore size is 17 μm, the depth of the "well" is 4 μm.

During the experiment, a microstructured layer with a pore size of 17 μm and a height of 4 μm produced 0.9 pL of microdroplets. **Figure 5.4** shows its microstructure diagram.

## 5.5 Discussions

The results presented in **Figure 5.3** indicate that without the application of voltage, the liquid does not enter the "well" and form droplets. This is attributed to the strong surface tension of water, which resists the entry of liquid into narrow channels. This observation is consistent with the behavior of liquid at the interface, as shown in **Figure**

**5.1**. Similar findings have been reported by Men et al., where they observed low droplet occupancy in small wells with a volume of 36 fL. [85] In their study, only 8.7% of the wells contained droplets. Therefore, there is a need to improve the occupancy of the "well" in this experimental setup. [85]

To address the challenge of low droplet occupancy, the principle of EWOD can be employed to temporarily reduce the surface tension in the local area and facilitate the entry of liquid into the "well". By applying voltage, the surface tension at the interface can be modified, allowing the liquid to overcome the resistance and enter the confined space. Subsequently, the PDMS cover can be applied to seal the device and remove excess liquid, as depicted in **Figure 5.5**(b) and (b').

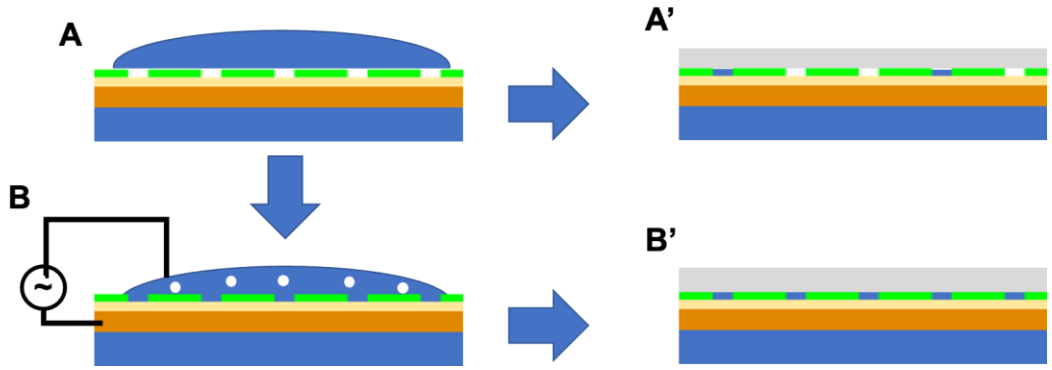


**Figure 5.5** Cross-section simulation of droplet generation chip (a) Liquid is added to the microstructure layer, the liquid does not enter the "well", and air is trapped in the "well" (a') Covered with PDMS without applying voltage , most of the "wells" have no liquid (b) add the liquid on the microstructure layer and drag the voltage, the air in the "well" is forced to go (b') After the air is removed, cover the PDMS, most of the The "well" contains liquid, forming a large number of tiny droplets.

This discussion highlights the importance of utilizing the EWOD principle to enhance droplet formation in small wells. By leveraging the control of surface tension through voltage application, the occupancy of the "well" can be improved, leading to more efficient droplet generation. Further optimization of the experimental setup and parameters can be explored to enhance the droplet occupancy rate and fine-tune the droplet volume for specific applications.

## 5.6 Further applications

The utilization of micro-droplets has significant potential in various fields,

including microalgae culturing, medical testing applications, and trace substance detection.

**Microalgae culturing**

Microalgae screening and cultivation require the use of droplet digital microfluidics. With the ability to create pL droplets, it becomes possible to encapsulate individual microalgae within droplets. This enables precise control and isolation of microalgae, allowing for efficient screening and cultivation processes. **Figure 5.6** demonstrates the successful separation of microalgae into individual droplets using the experimental setup.

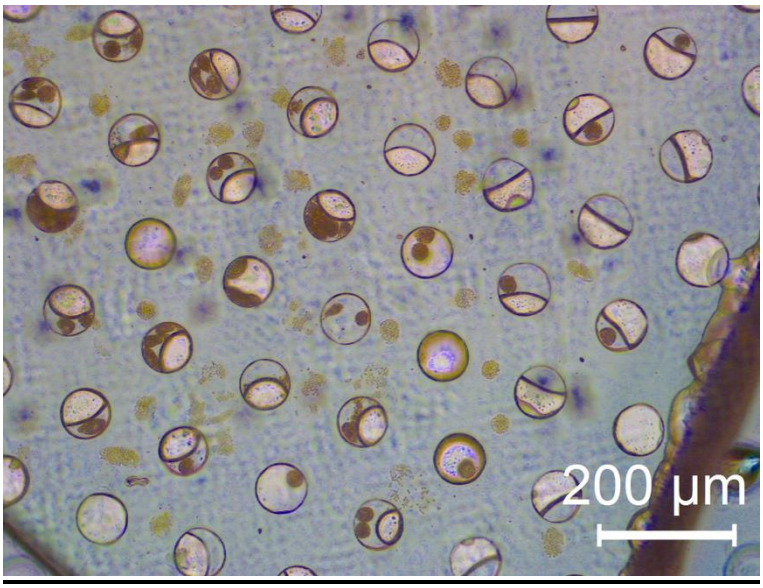


**Figure 5.6** Microalgae in microdroplet.

**Medical testing application**

Traditional medical testing often involves collecting relatively large volumes of samples using hands and pipettes. However, by utilizing micro-droplets, it becomes feasible to divide the sample volume into smaller sections. This concentration of the target substance in each droplet enhances the sensitivity of detection. In the case of virus detection, this can be particularly valuable in identifying low concentrations of viruses in patient samples, thereby improving detection capabilities.

**Trace substance detection application**

Micro-droplets also hold promise in the detection of trace substances. Different compounds have specific lower limits for identification in forensic testing and drug analysis. By reducing the volume of each liquid sample and concentrating the target substance within each droplet, the lower detection limit can be significantly improved. The production of micro-droplets will play a crucial role in advancing technologies related to trace substance detection.

These future applications demonstrate the potential impact and versatility of micro-droplets in various fields. As the technology continues to evolve, further advancements in droplet generation techniques and the integration of digital microfluidics will enable more precise and efficient processes in microalgae culturing, medical testing, and trace substance detection.

## 5.7 Summary

The use of micro-droplets in digital microfluidics offers significant potential for various applications. The ability to generate droplets of precise size and shape enables enhanced control and manipulation of samples at the microscale. Through experimental methods, successful creation of EWOD templated microstructured layers and generation of 0.9 pL micro-droplets have been demonstrated. Future applications include microalgae culturing, medical testing, and trace substance detection. These applications benefit from the precise control and concentration capabilities of micro-droplets. Continued research in this field promises advancements in biotechnology, healthcare, and forensic analysis, paving the way for improved diagnostics, drug discovery, and environmental monitoring.

# Chapter 6 Conclusions and Future Work

In conclusion, this dissertation has made significant contributions to the field of digital microfluidics for droplet manipulation and generation. Through a comprehensive literature review, the potential applications and challenges in microalgae screening and cultivation were identified. The research then focused on developing an innovative approach to reduce the number of control electrodes in droplet digital microfluidics using crisscross electrodes, resulting in the successful production of a 16×16-channel control electrode chip, providing 256 control units.

Furthermore, the dissertation addressed the limitation of surface tension in producing small droplets and successfully achieved the rapid generation of pL-sized droplets. The developed method demonstrated the production of droplets with a volume as low as 0.9 pL, a significant improvement compared to previous literature reports.

These advancements have far-reaching implications for various applications. The reduced number of control electrodes in the 16×16-channel chip enhances the scalability and potential for high-throughput droplet manipulation. The ability to generate pL-sized droplets opens up new possibilities in microalgae culturing, medical testing, and trace substance detection, offering higher sensitivity and improved detection limits.

Looking ahead, future research directions may include further optimization of the electrode configuration and control algorithms to enhance droplet manipulation efficiency. Additionally, exploring the scalability and integration of the developed techniques with other microfluidic functionalities can lead to the development of more sophisticated and versatile droplet-based systems.

Overall, this dissertation's achievements in reducing control electrodes and rapidly generating pL-sized droplets pave the way for more efficient and precise applications in the fields of biotechnology, diagnostics, and beyond. The 16×16-channel control electrode chip with 256 control units and the production of 0.9 pL of droplets demonstrate the potential for advancements in high-throughput droplet manipulation and enable breakthroughs in various applications requiring precise droplet control.

In future research, further improvements can be made in the control of the chip. The following are some examples: how to make the droplet more stable in the chip, reduce the contamination of the droplet in the hydrophobic layer of the chip, and how to extract the droplet hidden in the microstructure layer into the channel.

Sine the surface of the top and bottom plates has been coated hydrophobic layer, the liquid is in an unstable state for a long time. If it vibrates, or if the upper and lower layers of the chip are not perfectly level, the liquid has a chance to move to the wider side. This is because the upper and lower space is relatively wide, and relatively, the

force of the liquid droplet being squeezed will be relatively small.

This situation often occurs in the first experiment. Therefore, double electrodes can be used, as shown in **Figure 6.1**. When the droplet does not need to be moved, the smaller electrode will apply a voltage, similar with virtual pins are applied to the four directions of the droplet, so that the liquid is fixed in the relevant control unit.

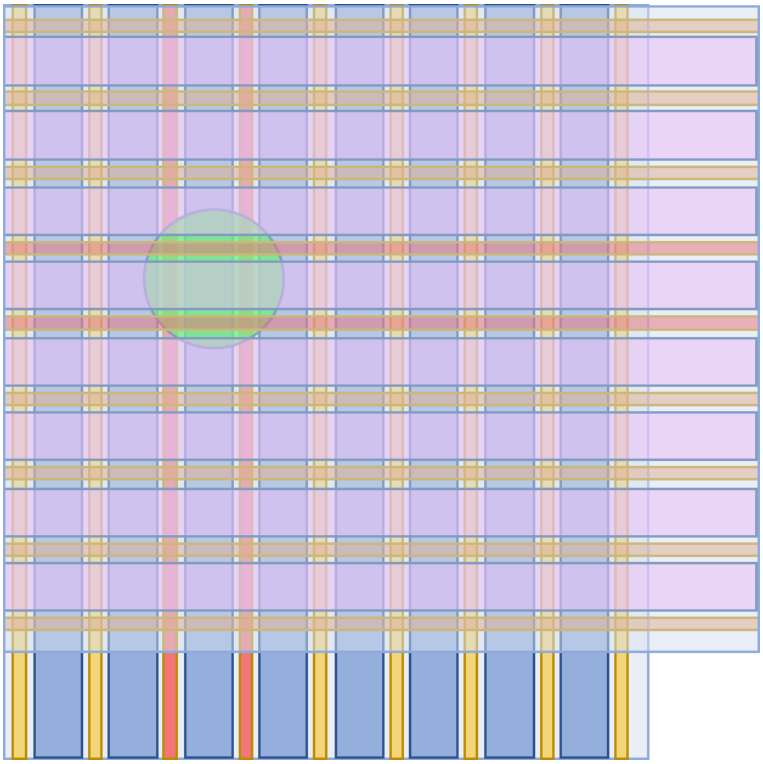

**Figure 6.1** Illustration of using double electrodes (virtual pin) for droplet stabilization in the microfluidic chip.

In the medical detection droplet digital microfluidic chip, samples often contaminate the hydrophobic layer. Therefore, the development of a replaceable hydrophobic layer

will greatly reduce the waste of the chip.

Because flush and water are two liquid phases that cannot mix, the microstructure layer can be used to fix the oil on the substrate, and then let the water move on it. **Figure 6.2** is a related schematic diagram. When the water droplets remain in the oil, a large amount of oil can be used to wash away the polluted oil, so that the purpose of replacing the pond can be achieved.

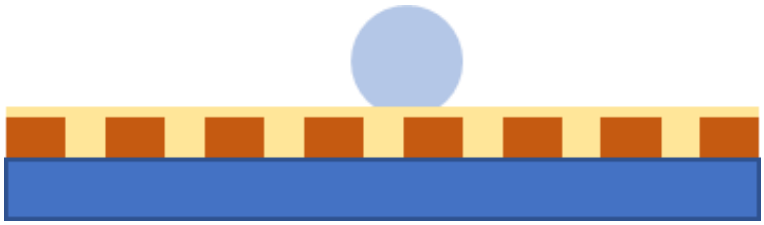

**Figure 6.2** Schematic diagram illustrating the use of a microstructure layer for extracting water droplets from the oil phase, allowing for replacement of the hydrophobic layer.

For extracting the liquid hidden in the microstructure layer to the channel, this needs to break through the surface tension again. This can use ultrasonic vibrations or localized heating to change the form of the liquid and enable its escape from the microstructure layer.

In future research, exploring these areas will contribute to enhancing the performance and capabilities of droplet digital microfluidic systems, enabling more stable droplet manipulation, reduced contamination, and efficient extraction of hidden droplets.

# Reference

[1] R.Powers andJ. C.Copeland, *Encyclopedia of Biophysics*. Springer Berlin, Heidelberg, 2013.

[2] A.Xu andP.Li, "Microfluidic Device Control System Based on Segmented Temperature Sensor," *Mob. Inf. Syst.*, vol. 2021, 2021, doi: 10.1155/2021/9930649.

[3] X.Wang, J.Zhu, C.Yang, F.Qin, andB.Zhang, "Segmented Microfluidics-Based Packing Technology for Chromatographic Columns," *Anal. Chem.*, vol. 93, no. 24, pp. 8450–8458, 2021, doi: 10.1021/acs.analchem.1c00545.

[4] C. D.Ahrberg, A.Manz, andB. G.Chung, "Polymerase chain reaction in microfluidic devices," *Lab Chip*, vol. 16, no. 20, pp. 3866–3884, 2016, doi: 10.1039/c6lc00984k.

[5] C.Zhang, J.Xu, W.Ma, andW.Zheng, "PCR microfluidic devices for DNA amplification," *Biotechnol. Adv.*, vol. 24, no. 3, pp. 243–284, 2006, doi: 10.1016/j.biotechadv.2005.10.002.

[6] E.Huang, Y.Wang, N.Yang, B.Shu, G.Zhang, andD.Liu, "A fully automated microfluidic PCR-array system for rapid detection of multiple respiratory tract infection pathogens," *Anal. Bioanal. Chem.*, vol. 413, no. 7, pp. 1787–1798,

2021, doi: 10.1007/s00216-021-03171-4.

[7] J. A.Berkenbrock, R.Grecco-Machado, andS.Achenbach, “Microfluidic devices for the detection of viruses: Aspects of emergency fabrication during the COVID-19 pandemic and other outbreaks,” *Proc. R. Soc. A Math. Phys. Eng. Sci.*, vol. 476, no. 2243, 2020, doi: 10.1098/rspa.2020.0398.

[8] E. A.Tarim *et al.*, “Microfluidic-based virus detection methods for respiratory diseases,” *Emergent Mater.*, vol. 4, no. 1, pp. 143–168, 2021, doi: 10.1007/s42247-021-00169-7.

[9] S.Yang, S.Lv, W.Zhang, andY.Cui, “A Review of Opportunities and Challenges,” *Sensors*, vol. 22, 2022, doi: 10.3390/s22041620.

[10] M. R.Jamiruddin *et al.*, “Microfluidics Technology in SARS-CoV-2 Diagnosis and Beyond: A Systematic Review,” *Life*, vol. 12, no. 5, pp. 1–32, 2022, doi: 10.3390/life12050649.

[11] M.Sun *et al.*, “Paper-based microfluidic chip for rapid detection of SARS-CoV-2 N protein,” *Bioengineered*, vol. 13, no. 1, pp. 876–883, 2022, doi: 10.1080/21655979.2021.2014385.

[12] B.Yin, X.Wan, A. S. M. M. F.Sohan, andX.Lin, “Microfluidics-Based POCT for SARS-CoV-2 Diagnostics,” *Micromachines*, vol. 13, no. 8, 2022, doi: 10.3390/mi13081238.

[13] M.Wu *et al.*, "Microfluidic particle dam for direct visualization of SARS-CoV-2 antibody levels in COVID-19 vaccinees," *Sci. Adv.*, vol. 8, no. 22, pp. 1–12, 2022, doi: 10.1126/sciadv.abn6064.

[14] J.Zhai *et al.*, "Cancer drug screening with an on-chip multi-drug dispenser in digital microfluidics," *Lab Chip*, vol. 21, no. 24, pp. 4749–4759, 2021, doi: 10.1039/d1lc00895a.

[15] X.Zhang, X.Lu, W.Gao, Y.Wang, C.Jia, andH.Cong, "A label-free microfluidic chip for the highly selective isolation of single and cluster CTCs from breast cancer patients," *Transl. Oncol.*, vol. 14, no. 1, 2021, doi: 10.1016/j.tranon.2020.100959.

[16] Q. R.Guo *et al.*, "Multifunctional microfluidic chip for cancer diagnosis and treatment," *Nanotheranostics*, vol. 5, no. 1, pp. 73–89, 2021, doi: 10.7150/ntno.49614.

[17] D.Millington, S.Norton, R.Singh, R.Sista, V.Srinivasan, andV.Pamula, "Digital microfluidics comes of age: high-throughput screening to bedside diagnostic testing for genetic disorders in newborns," *Expert Rev. Mol. Diagn.*, vol. 18, no. 8, pp. 701–712, 2018, doi: 10.1080/14737159.2018.1495076.

[18] E.Liu, C.Wang, H.Zheng, S.Song, A.Riaud, andJ.Zhou, "Two-dimensional manipulation of droplets on a single-sided continuous optoelectrowetting digital

microfluidic chip," *Sensors Actuators B Chem.*, vol. 368, no. 17, 2022, doi: 10.1016/j.snb.2022.132231.

[19] M.Torabinia, U. S.Dakarapu, P.Asgari, J.Jeon, andH.Moon, "Electrowetting-on-dielectric (EWOD) digital microfluidic device for in-line workup in organic reactions: A critical step in the drug discovery work cycle," *Sensors Actuators, B Chem.*, vol. 330, no. August 2020, p. 129252, 2021, doi: 10.1016/j.snb.2020.129252.

[20] C.Peng, Z.Zhang, C. J.Kim, andY. S.Ju, "EWOD (electrowetting on dielectric) digital microfluidics powered by finger actuation," *Lab Chip*, vol. 14, no. 6, pp. 1117–1122, 2014, doi: 10.1039/c3lc51223a.

[21] D.Huang, K.Wang, Y.Wang, H.Sun, X.Liang, andT.Meng, "Precise control for the size of droplet in T-junction microfluidic based on iterative learning method," *J. Franklin Inst.*, vol. 357, no. 9, pp. 5302–5316, 2020, doi: 10.1016/j.jfranklin.2020.02.046.

[22] C.Dong *et al.*, "A 3D microblade structure for precise and parallel droplet splitting on digital microfluidic chips," *Lab Chip*, vol. 17, no. 5, pp. 896–904, 2017, doi: 10.1039/C6LC01539E.

[23] S. K.Cho, Y.Zhao, andC. J.Kim, "Concentration and binary separation of micro particles for droplet-based digital microfluidics," *Lab Chip*, vol. 7, no. 4, pp.

490–498, 2007, doi: 10.1039/b615665g.

[24] P.Zhu andL.Wang, “Passive and active droplet generation with microfluidics: a review,” *Lab Chip*, vol. 17, no. 1, pp. 34–75, 2017, doi: 10.1039/C6LC01018K.

[25] C.Fuentes-Grünewald, E.Garcés, E.Alacid, N.Sampedro, S.Rossi, andJ.Camp, “Improvement of lipid production in the marine strains Alexandrium minutum and Heterosigma akashiwo by utilizing abiotic parameters,” *J. Ind. Microbiol. Biotechnol.*, vol. 39, no. 1, pp. 207–216, 2012, doi: 10.1007/s10295-011-1016-6.

[26] M. D.Guiry, “How many species of algae are there?,” *J. Phycol.*, vol. 48, no. 5, pp. 1057–1063, 2012, doi: 10.1111/j.1529-8817.2012.01222.x.

[27] L.Zhu, “Biorefinery as a promising approach to promote microalgae industry: An innovative framework,” *Renew. Sustain. Energy Rev.*, vol. 41, pp. 1376–1384, 2015, doi: 10.1016/j.rser.2014.09.040.

[28] T. M.Mata, A. A.Martins, andN. S.Caetano, “Microalgae for biodiesel production and other applications: A review,” *Renew. Sustain. Energy Rev.*, vol. 14, no. 1, pp. 217–232, 2010, doi: 10.1016/j.rser.2009.07.020.

[29] L.Brennan andP.Owende, “Biofuels from microalgae-A review of technologies for production, processing, and extractions of biofuels and co-products,” *Renew. Sustain. Energy Rev.*, vol. 14, no. 2, pp. 557–577, 2010, doi:

10.1016/j.rser.2009.10.009.

[30] T.Mutanda, D.Ramesh, S.Karthikeyan, S.Kumari, A.Anandraj, andF.Bux, "Bioprospecting for hyper-lipid producing microalgal strains for sustainable biofuel production," *Bioresour. Technol.*, vol. 102, no. 1, pp. 57–70, 2011, doi: 10.1016/j.biortech.2010.06.077.

[31] A.Han, H.Hou, L.Li, H. S.Kim, andP.deFigueiredo, "Microfabricated devices in microbial bioenergy sciences," *Trends Biotechnol.*, vol. 31, no. 4, pp. 225–232, 2013, doi: 10.1016/j.tibtech.2012.12.002.

[32] G. M.Whitesides, "What comes next?," *Lab Chip*, vol. 11, no. 2, pp. 191–193, 2011, doi: 10.1039/c0lc90101f.

[33] G. B.Salieb-Beugelaar, G.Simone, A.Arora, A.Philippi, andA.Manz, "Latest developments in microfluidic cell biology and analysis systems," *Anal. Chem.*, vol. 82, no. 12, pp. 4848–4864, 2010, doi: 10.1021/ac1009707.

[34] A.Grünberger, W.Wiechert, andD.Kohlheyer, "Single-cell microfluidics: Opportunity for bioprocess development," *Curr. Opin. Biotechnol.*, vol. 29, no. 1, pp. 15–23, 2014, doi: 10.1016/j.copbio.2014.02.008.

[35] Z.Zhu andC. J.Yang, "Hydrogel droplet microfluidics for high-throughput single molecule/cell analysis," *Acc. Chem. Res.*, vol. 50, no. 1, pp. 22–31, 2017, doi: 10.1021/acs.accounts.6b00370.

[36] T. S.Kaminski, O.Scheler, andP.Garstecki, "Droplet microfluidics for microbiology: Techniques, applications and challenges," *Lab Chip*, vol. 16, no. 12, pp. 2168–2187, 2016, doi: 10.1039/c6lc00367b.

[37] L.Shang, Y.Cheng, andY.Zhao, "Emerging Droplet Microfluidics," *Chem. Rev.*, vol. 117, no. 12, pp. 7964–8040, 2017, doi: 10.1021/acs.chemrev.6b00848.

[38] T.Encarnação *et al.*, "Monitoring oil production for biobased feedstock in the microalga Nannochloropsis sp.: a novel method combining the BODIPY BD-C12 fluorescent probe and simple image processing," *J. Appl. Phycol.*, vol. 30, no. 4, pp. 2273–2285, 2018, doi: 10.1007/s10811-018-1437-y.

[39] P.Bodénès, H. Y.Wang, T. H.Lee, H. Y.Chen, andC. Y.Wang, "Microfluidic techniques for enhancing biofuel and biorefinery industry based on microalgae," *Biotechnol. Biofuels*, vol. 12, no. 1, pp. 1–25, 2019, doi: 10.1186/s13068-019-1369-z.

[40] W. H.Xie *et al.*, "Construction of Novel Chloroplast Expression Vector and Development of an Efficient Transformation System for the Diatom Phaeodactylum tricornutum," *Mar. Biotechnol.*, vol. 16, no. 5, pp. 538–546, 2014, doi: 10.1007/s10126-014-9570-3.

[41] T.Moses, P.Mehrshahi, A. G.Smith, andA.Goossens, "Synthetic biology approaches for the production of plant metabolites in unicellular organisms," *J.*

*Exp. Bot.*, vol. 68, no. 15, pp. 4057–4074, 2017, doi: 10.1093/jxb/erx119.

[42] M. A.Scranton *et al.*, "Synthetic promoters capable of driving robust nuclear gene expression in the green alga Chlamydomonas reinhardtii," *Algal Res.*, vol. 15, pp. 135–142, 2016, doi: 10.1016/j.algal.2016.02.011.

[43] P.Crozet *et al.*, "Birth of a Photosynthetic Chassis: A MoClo Toolkit Enabling Synthetic Biology in the Microalga Chlamydomonas reinhardtii," *ACS Synth. Biol.*, vol. 7, no. 9, pp. 2074–2086, 2018, doi: 10.1021/acssynbio.8b00251.

[44] M.Li, M.VanZee, K.Goda, andD.DiCarlo, "Size-based sorting of hydrogel droplets using inertial microfluidics," *Lab Chip*, vol. 18, no. 17, pp. 2575–2582, 2018, doi: 10.1039/c8lc00568k.

[45] Z.Yu *et al.*, "Droplet-based microfluidic screening and sorting of microalgal populations for strain engineering applications," *Algal Res.*, vol. 56, 2021, doi: 10.1016/j.algal.2021.102293.

[46] M.Shakeel Syed, M.Rafeie, R.Henderson, D.Vandamme, M.Asadnia, andM.Ebrahimi Warkiani, "A 3D-printed mini-hydrocyclone for high throughput particle separation: Application to primary harvesting of microalgae," *Lab Chip*, vol. 17, no. 14, pp. 2459–2469, 2017, doi: 10.1039/c7lc00294g.

[47] C.Two, "Electrostatics and Dielectrics," in *AC Electrokinetics : Colloids and Nanoparticles*, vol. 2, Hertfordshire, England : Research Studies Press, 2003.

[48] Z.Zhang, Y.Luo, X.Nie, D.Yu, andX.Xing, "A one-step molded microfluidic chip featuring a two-layer silver-PDMS microelectrode for dielectrophoretic cell separation," *Analyst*, vol. 145, no. 16, pp. 5603–5614, 2020, doi: 10.1039/d0an01085e.

[49] S. I.Han, H. S.Kim, K. H.Han, andA.Han, "Digital quantification and selection of high-lipid-producing microalgae through a lateral dielectrophoresis-based microfluidic platform," *Lab Chip*, vol. 19, no. 24, pp. 4128–4138, 2019, doi: 10.1039/c9lc00850k.

[50] B.Guo *et al.*, "High-throughput, label-free, single-cell, microalgal lipid screening by machine-learning-equipped optofluidic time-stretch quantitative phase microscopy," *Cytom. Part A*, vol. 91, no. 5, pp. 494–502, 2017, doi: 10.1002/cyto.a.23084.

[51] K.Hiramatsu *et al.*, "High-throughput label-free molecular fingerprinting flow cytometry," *Sci. Adv.*, vol. 5, no. 1, pp. 1–9, 2019, doi: 10.1126/sciadv.aau0241.

[52] Y.Wang, X.Wang, T.Pan, B.Li, andJ.Chu, "Label-free single-cell isolation enabled by microfluidic impact printing and real-time cellular recognition," *Lab Chip*, vol. 21, no. 19, pp. 3695–3706, 2021, doi: 10.1039/d1lc00326g.

[53] A.Aghakhani, H.Cetin, P.Erkoc, G. I.Tombak, andM.Sitti, "Flexural wave-based soft attractor walls for trapping microparticles and cells," *Lab Chip*, vol. 21, no.

3, pp. 582–596, 2021, doi: 10.1039/d0lc00865f.

[54] M.Navi, N.Abbasi, M.Jeyhani, V.Gnyawali, andS. S. H.Tsai, “Microfluidic diamagnetic water-in-water droplets: a biocompatible cell encapsulation and manipulation platform,” *Lab Chip*, vol. 18, no. 22, pp. 3361–3370, 2018, doi: 10.1039/C8LC00867A.

[55] G.Zheng *et al.*, “Development of Microfluidic Dilution Network-Based System for Lab-on-a-Chip Microalgal Bioassays,” *Anal. Chem.*, vol. 90, no. 22, pp. 13280–13289, 2018, doi: 10.1021/acs.analchem.8b02597.

[56] F.Liu, M.Yazdani, B. A.Ahner, andM.Wu, “An array microhabitat device with dual gradients revealed synergistic roles of nitrogen and phosphorous in the growth of microalgae,” *Lab Chip*, vol. 20, no. 4, pp. 798–805, 2020, doi: 10.1039/c9lc01153f.

[57] H. M.Saad, Marwa Gamal ; Selahi, Amirali ; Zoromba, Mohamed Shafick ; Mekki, Laila ; El-Bana, Magdy ; Dosoky, Noura S. ; Nobles, David ; Shafik, “A droplet-based gradient microfluidic to monitor and evaluate the growth of Chlorella vulgaris under different levels of nitrogen and temperatures,” *Algal Res.*, vol. 44, 2019, doi: 10.1016/j.algal.2019.101657.

[58] M.Andersson, S.Johansson, H.Bergman, L.Xiao, L.Behrendt, andM.Tenje, “A microscopy-compatible temperature regulation system for single-cell phenotype

analysis-demonstrated by thermoresponse mapping of microalgae," *Lab Chip*, vol. 21, no. 9, pp. 1694–1705, 2021, doi: 10.1039/d0lc01288b.

[59] M. G.Saad *et al.*, "High-throughput screening of Chlorella Vulgaris growth kinetics inside a droplet-based microfluidic device under irradiance and nitrate stress conditions," *Biomolecules*, vol. 9, no. 7, pp. 1–11, 2019, doi: 10.3390/biom9070276.

[60] Z.Xu, Y.Wang, Y.Chen, M. H.Spalding, andL.Dong, "Microfluidic chip for automated screening of carbon dioxide conditions for microalgal cell growth," *Biomicrofluidics*, vol. 11, no. 6, pp. 1–9, 2017, doi: 10.1063/1.5012508.

[61] S. K.Min, G. H.Yoon, J. H.Joo, S. J.Sim, andH. S.Shin, "Mechanosensitive physiology of chlamydomonas reinhardtii under direct membrane distortion," *Sci. Rep.*, vol. 4, pp. 1–9, 2014, doi: 10.1038/srep04675.

[62] J.Yao, H. S.Kim, J. Y.Kim, Y. E.Choi, andJ.Park, "Mechanical stress induced astaxanthin accumulation of: H. pluvialis on a chip," *Lab Chip*, vol. 20, no. 3, pp. 647–654, 2020, doi: 10.1039/c9lc01030k.

[63] G.Hardin, "The Competitive Exclusion Principle Published by : American Association for the Advancement of Science," *Science (80-. ).*, vol. 131, no. 3409, pp. 1292–1297, 1960, [Online]. Available: https://www.jstor.org/stable/1705965.

[64] D. N.Carruthers, C. K.Byun, B. J.Cardinale, andX. N.Lin, "Demonstration of

transgressive overyielding of algal mixed cultures in microdroplets," *Integr. Biol.*, vol. 9, no. 8, pp. 687–694, 2017, doi: 10.1039/c6ib00241b.

[65] T.Verburg, A.Schaap, S.Zhang, J.denToonder, andY.Wang, "Enhancement of microalgae growth using magnetic artificial cilia," *Biotechnol. Bioeng.*, vol. 118, no. 7, pp. 2472–2481, 2021, doi: 10.1002/bit.27756.

[66] B. J.Kim, L.V.Richter, N.Hatter, C. K.Tung, B. A.Ahner, andM.Wu, "An array microhabitat system for high throughput studies of microalgal growth under controlled nutrient gradients," *Lab Chip*, vol. 15, no. 18, pp. 3687–3694, 2015, doi: 10.1039/c5lc00727e.

[67] S. K. Fan *et al.*, "Manipulation of multiple droplets on N×M grid by cross-reference EWOD driving scheme and pressure-contact packaging," *Proc. IEEE Int. Conf. Micro Electro Mech. Syst.*, pp. 694–697, 2003, doi: 10.1109/MEMSYS.2003.1189844.

[68] M.VanZee *et al.*, "High-throughput selection of cells based on accumulated growth and division using PicoShell particles," in *Proceedings of the National Academy of Sciences of the United States of America*, 2022, vol. 119, no. 4, doi: 10.1073/pnas.2109430119.

[68] H.Geng, J.Feng, L. M.Stabryla, andS. K.Cho, "Dielectrowetting manipulation for digital microfluidics: creating, transporting, splitting, and merging of

droplets," *Lab Chip*, vol. 17, no. 6, pp. 1060–1068, 2017, doi: 10.1039/c7lc00006e.

[69] B.Hadwen *et al.*, "Programmable large area digital microfluidic array with integrated droplet sensing for bioassays," *Lab Chip*, vol. 12, no. 18, pp. 3305–3313, 2012, doi: 10.1039/c2lc40273d.

[70] J.Li andC. J.Kim, "Current commercialization status of electrowetting-on-dielectric (EWOD) digital microfluidics," *Lab Chip*, vol. 20, no. 10, pp. 1705–1712, 2020, doi: 10.1039/d0lc00144a.

[71] H. H.Jeong, B.Lee, S. H.Jin, S. G.Jeong, andC. S.Lee, "A highly addressable static droplet array enabling digital control of a single droplet at pico-volume resolution," *Lab Chip*, vol. 16, no. 9, pp. 1698–1707, 2016, doi: 10.1039/c6lc00212a.

[72] A.Tong, Q. L.Pham, V.Shah, A.Naik, P.Abatemarco, andR.Voronov, "Automated Addressable Microfluidic Device for Minimally Disruptive Manipulation of Cells and Fluids within Living Cultures," *ACS Biomater. Sci. Eng.*, vol. 6, no. 3, pp. 1809–1820, 2020, doi: 10.1021/acsbiomaterials.9b01969.

[73] S.-Y. Park and P.-Y. Chiou, "Light-Driven Droplet Manipulation Technologies for Lab-on-a-Chip Applications," *Advances in OptoElectronics (Hindawi)*, vol. 2011, pp. 1–12, 2011, doi: 10.1155/2011/909174.

[74] S. N.Pei, J. K.Valley, Y. L.Wang, andM. C.Wu, “Distributed Circuit Model for Multi-Color Light-Actuated Opto-Electrowetting Microfluidic Device,” *J. Light. Technol.*, vol. 33, no. 16, pp. 3486–3493, 2015, doi: 10.1109/JLT.2015.2405076.

[75] H. Y.Hsu, A. T.Ohta, P. Y.Chiou, A.Jamshidi, S. L.Neale, andM. C.Wu, “Phototransistor-based optoelectronic tweezers for dynamic cell manipulation in cell culture media,” *Lab Chip*, vol. 10, no. 2, pp. 165–172, 2010, doi: 10.1039/b906593h.

[76] Y.Yang, Y.Mao, K. S.Shin, C. O.Chui, andP. Y.Chiou, “Self-Locking Optoelectronic Tweezers for Single-Cell and Microparticle Manipulation across a Large Area in High Conductivity Media,” *Sci. Rep.*, vol. 6, no. February, pp. 4–11, 2016, doi: 10.1038/srep22630.

[77] J. C.Ndukaife, A.V.Kildishev, A. G. A.Nnanna, V. M.Shalaev, S. T.Wereley, andA.Boltasseva, “Long-range and rapid transport of individual nano-objects by a hybrid electrothermoplasmonic nanotweezer,” *Nat. Nanotechnol.*, vol. 11, no. 1, pp. 53–59, 2016, doi: 10.1038/nnano.2015.248.

[78] R. Pethig, Dielectrophoresis: Status of the theory, technology, and applications, Biomicrofluidics, 4 (2010) 022811.

[79] B. Çetin, D. Li, Dielectrophoresis in microfluidics technology, Electrophoresis,

32 (2011) 2410-2427

[80] J. B.Chae, S. J.Lee, J.Yang, andS. K.Chung, "3D electrowetting-on-dielectric actuation," *Sensors Actuators, A Phys.*, vol. 234, pp. 331–338, 2015, doi: 10.1016/j.sna.2015.09.004.

[81] L.Barsanti *et al.*, "In vivo absorption spectra of the two stable states of the Euglena photoreceptor photocycle," *Photochem. Photobiol.*, vol. 85, no. 1, pp. 304–312, 2009, doi: 10.1111/j.1751-1097.2008.00438.x.

[82] G. K. Strother. and J.J. andBiophyAical, "In vivo Absorption Spectra of Euglena: Chloroplast and Eyespot," *J. Protozool.*, vol. 8, no. 3, pp. 261–265, 1961, doi: 10.4103/jispcd.JISPCD.

[83] R.Wang, L.Zhang, M.Gao, Q.Wang, Z.Deng, andL.Gui, "A liquid-metal-based dielectrophoretic microdroplet generator," *Micromachines*, vol. 10, no. 11, 2019, doi: 10.3390/mi10110769.

[84] D.Paulssen, W.Feng, I.Pini, andP. A.Levkin, "Formation of Liquid–Liquid Micropatterns through Guided Liquid Displacement on Liquid-Infused Surfaces," *Adv. Mater. Interfaces*, vol. 5, no. 18, pp. 1–8, 2018, doi: 10.1002/admi.201800852.

[85] Men, Y., Fu, Y., Chen, Z., Sims, P. A., Greenleaf, W. J., and Huang, Y., " Digital Polymerase Chain Reaction in an Array of Femtoliter Polydimethylsiloxane

Microreactors," *Analytical Chemistry* (Washington), vol. 84, no. 10, pp. 4262–4266, 2012, doi: 10.1021/ac300761n